JPRS-JST-93-004
28 JANUARY 1993

JPRS Report

Science & Technology

Japan

THE JRDC INTERNATIONAL SYMPOSIUM ON SUPERMOLECULES AND MOLECULAR SYSTEMS

JPRS-JST-93-004
28 JANUARY 1993

SCIENCE & TECHNOLOGY
JAPAN

THE JRDC INTERNATIONAL SYMPOSIUM ON SUPERMOLECULES AND MOLECULAR SYSTEMS

43070028 Fukuoka JRDC FUKUOKA PREFECTURE in English 25 Nov 92 pp 1-94

[Selected abstracts presented at the JRDC International Symposium on Supermolecules and Molecular Systems held 25-26 Nov 92 in Fukuoka, sponsored by the Research Development Corporation of Japan, Fukuoka Prefecture, and Kyushu University]

CONTENTS

Supermolecules, Molecular Systems

43070028A Fukuoka JRDC FUKUOKA PREFECTURE in English 25 Nov 92 pp i-ii

[Text] **Table of Contents**

25 November 1992 (Wed)

26 November 1992 (Thu)

Self, Nonself Recognition of Asymmetric Catalysts

43070028B Fukuoka JRDC FUKUOKA PREFECTURE in English 25 Nov 92 pp 3-7

[Article by Ryoji Noyori, Department of Chemistry, Nagoya University, director of Molecular Catalysis Project]

[Text] Molecules in a fluid solution cannot exist independently but have interaction with surrounding molecules, not only solvent but also other solute molecules. The partners may have the same, similar, or entirely different properties. The interaction often occurs via special molecular recognition which affects profoundly the chemical behavior. In certain asymmetric catalyses, the catalytic species causes self or nonself molecular recognition which exert remarkable effects on the stereoselectivities and velocity of the reaction.

Sterically constrained β-dialkylamino alcohols markedly accelerate nucleophilic addition of dialkylzincs to aldehydes. Use of a catalytic amount of (-)-3-*exo*-(dimethylamino)isoborneol [(-)-DAIB] effects highly enantioselective alkylation giving a diverse array of secondary alcohols in up to 99% ee.[1]

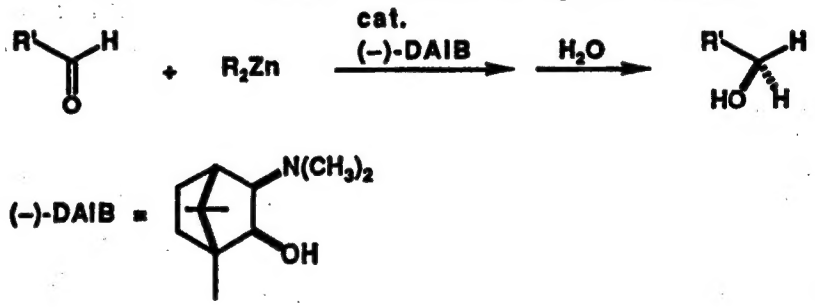

The stoichiometry of aldehyde, dialkylzinc, and DAIB auxiliary strongly affects the reactivity. Without DAIB, diethylzinc is inert to benzaldehyde in hydrocarbons at room temperature, but addition of 100 mol % of DAIB to diethylzinc does not cause ethylation either. The alkylation takes place only with a catalytic quantity (a few mol %) of DAIB.

This fact indicates that two Zn atoms per aldehyde participate in the transition state of the alkylation. Figure 1 outlines the possible mechanism. The kinetic study suggests that the intramolecular transformation, D → E, is the turnover-limiting and also stereo-determining step. Complexes A-D are in an equilibrium, where R is rapidly scrambling.

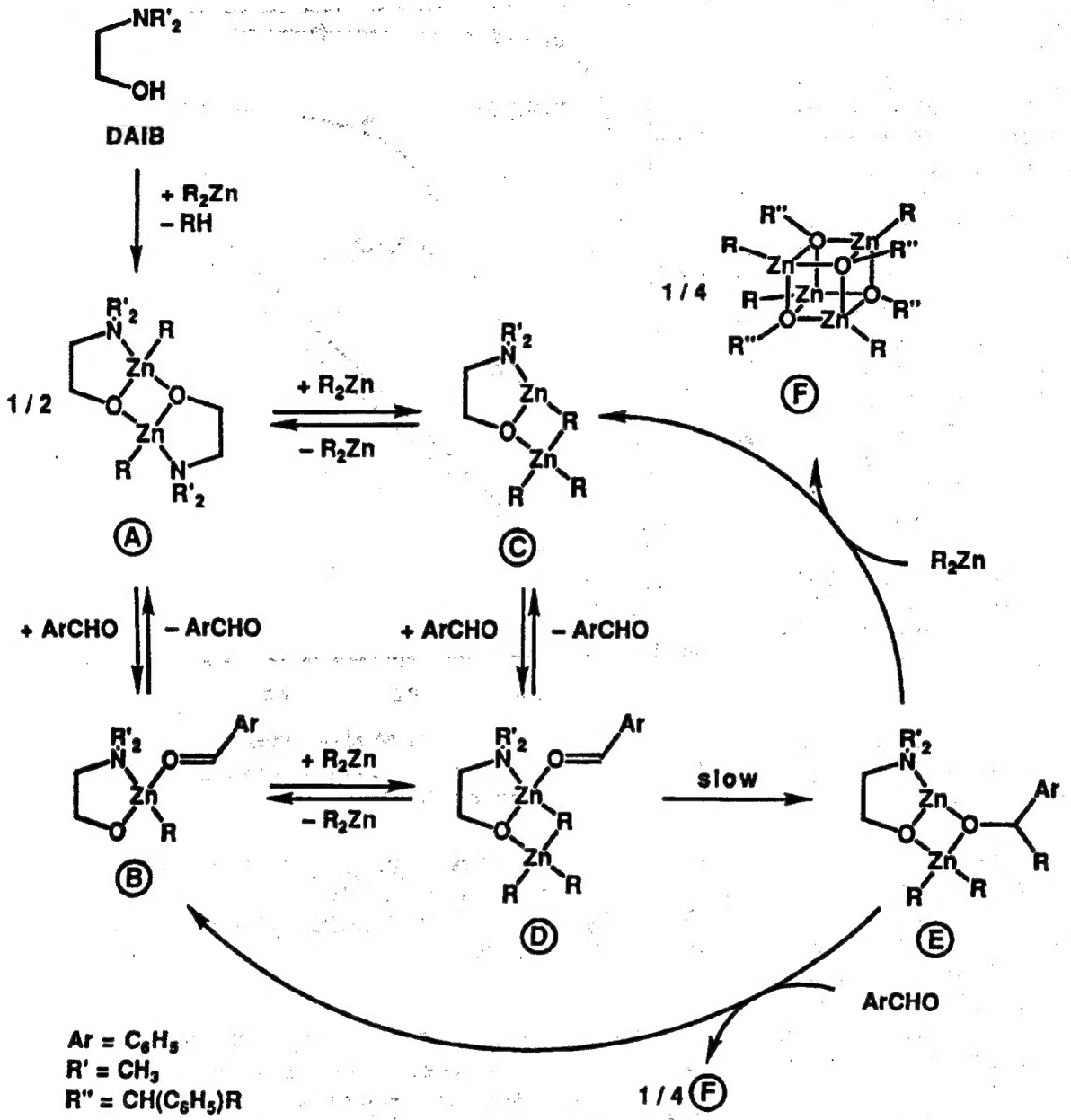

Figure 1. Catalytic Cycle of the DAIB Catalyzed Enantioselective Alkylation of Benzaldehyde

The well-shaped three-dimensional structure of DAIB is obviously the origin of the high degree of enantioselection but some kinetic parameters are suitably coupled to lead to the excellent catalytic chiral efficiency. First, the linear, unreactive dialkylzinc is transformed to a bent, reactive alkylzinc compound by modification by the amino alcohol. Steric congestion of DAIB facilitates the dissociation of **A** to the monomeric true catalyst. In addition, removal of the stable self-aggregate **F** from the catalytic cycle avoids product inhibition or any other adverse effects on the catalysis.

Reaction of benzaldehyde and diethylzinc with 8 mol % of optically pure (–)-DAIB in toluene affords the S ethylation product in 98% ee. Notably, the catalysis with (–)-DAIB in 14% ee [(–):(+) = 57:43] gives the same product in >95% ee. As shown in Figure 2, enormous chirality amplification is seen in the enantioselective methylation and ethylation reaction.

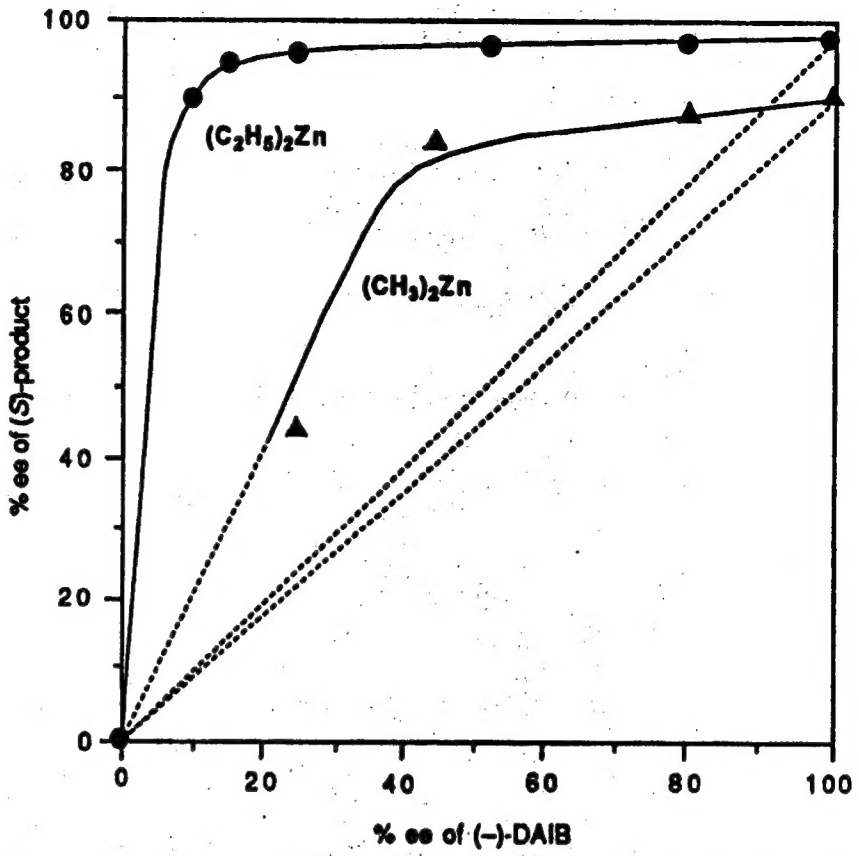

Figure 2. The ee of the Alkylation Product as a Function of the ee of DAIB

•Reaction using 0.42 M $(C_2H_5)_2Zn$, 0.42 M C_6H_5CHO, and 34 mM (–)-DAIB in toluene at 0°C

▲0.47 M $(CH_3)_2Zn$, 0.49 M C_6H_5CHO, 47 mM (–)-DAIB in toluene $-d_8$ at 32°C

The chiral catalyst system exhibits higher reactivity than the racemic catalyst system. Under certain conditions, the former is >600-times more reactive than the latter. The origin of this unusual effect has been elucidated at a molecular structure level. Reaction of equimolar amounts of enantiomerically pure (–)-DAIB and dimethylzinc forms (2S,2'S)-G (R = CH_3). The X-ray crystallographic analysis indicates that this dinuclear Zn compound has a C_2 symmetry and that the central 5/4/5 tricyclic system possesses a syn geometry (Figure 3). This compound, upon mixing with an equimolar amount of the (+)-DAIB-derived enantiomer, is instantaneously converted to (2S,2'R)-G (R = CH_3) that possesses a meso, anti 5/4/5 structure. The same dinuclear compound is obtained by reaction of racemic DAIB and dimethylzinc in a 1:1 molar ratio. This thermodynamic relationship is controlled by the strict matching of chirality as illustrated in Figure 4. The true catalyst for the enantioselective alkylation is monomeric (2S)- or (2R)-H. Their self or nonself recognition leads to diastereometric dinuclear complexes, where the heterochiral dinuclear complex (2S,2'R)-G is overwhelmingly stabler than the homochiral dinuclear complex, (2S,2'S)- or (2R,2'R)-G.

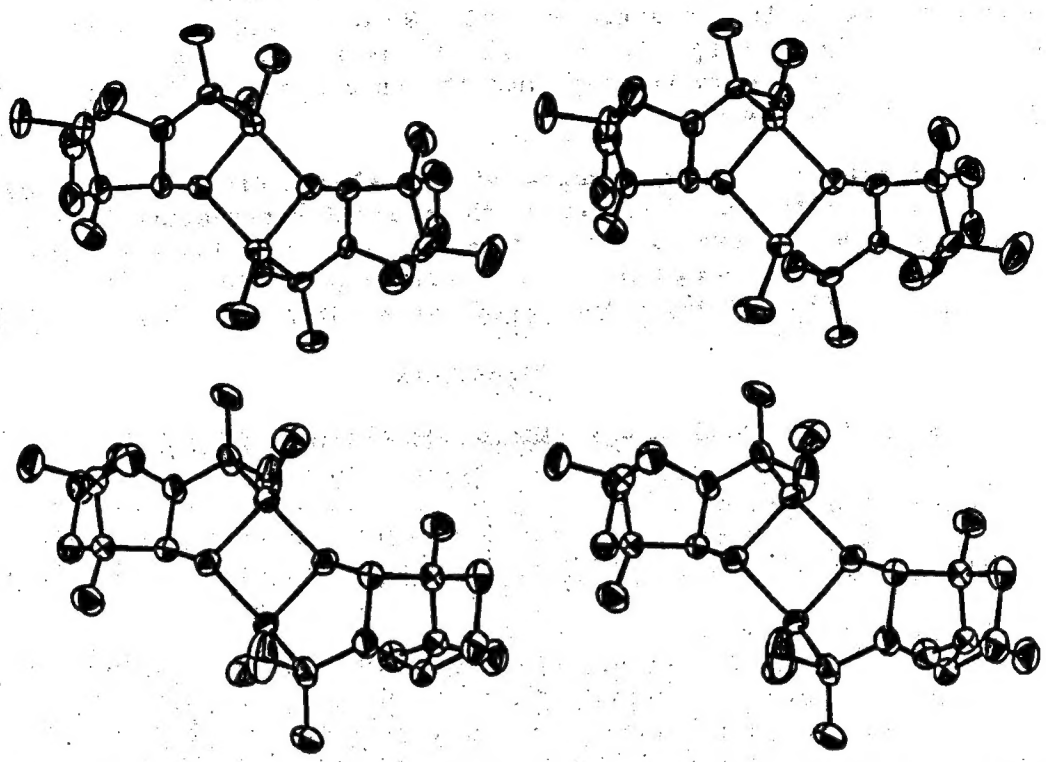

Figure 3. Stereoview of (2S,2'S)-G (upper) and (2S,2'R)-G (R = CH_3) (lower)

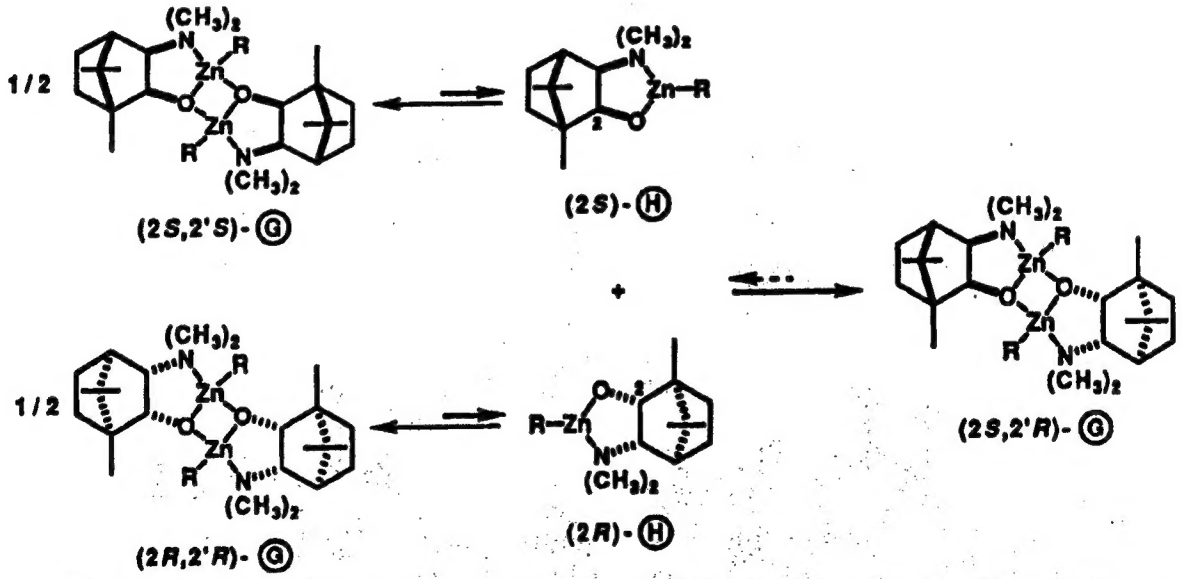

Figure 4. Enantiometer Recognition of Chiral Trigonal Zn Compounds

When partially resolved (-)-DAIB is used as auxiliary, all the minor enantiomer (2R)-H is converted to (2S,2'R)-G by taking the same amount of (2S)-H and the remaining (2S)-H forms the self dimer (2S,2'S)-G. The latter tends to dissociate more readily into the true catalyst (2S)-H, exhibiting a high turnover efficiency.

This is perhaps the first example of the elucidation of the mechanism of catalytic chirality amplification at the molecular structure level. Such self and nonself recognition is not limited to the enantiomeric catalysts. The chiral catalyst H recognizes the diastereomers to a different degree, resulting in various nonlinear effects in asymmetric catalysis.

References

1. R. Noyori and M. Kitamura, ANGEW. CHEM., INT. ED. ENGL., Vol 30 No 49, 1991.

Design of Calixarene-Based Supramolecules: From Theoretical Calculations to Self-Assemblies

43070028C Fukuoka JRDC FUKUOKA PREFECTURE in English 25 Nov 92 pp 9-13

[Article by Seiji Shinkai, Chemirecognics Project, ERATO, Research Development Corporation of Japan and Department of Chemical Science and Technology, Faculty of Engineering, Kyushu University]

[Text] **Introduction**

Calixarenes are cavity-shaped cyclic molecules made up of phenol units linked via alkylidene groups. In spite of their attractive architecture, studies of and applications to molecular recognition chemistry have been very limited. This shows a sharp contrast to cyclodextrins and crown ethers which can form a variety of host-guest-type solution complexes. The aim of our research project is to withdraw latent possibilities as functionalizable materials from a calixarene family and to apply them to molecular recognition, ion-sensing, etc.

On the Structural Characteristics of Calixarenes

Conformational freedom still remains in calixarene molecules, which is called "oxygen-through-the-annulus" rotation. This mobility is conveniently monitored by temperature-dependent ^{1}HNMR. We estimated the inversion energy to be 11-17 kcal mol^{-1} by the computational simulation of the spectra.[1]

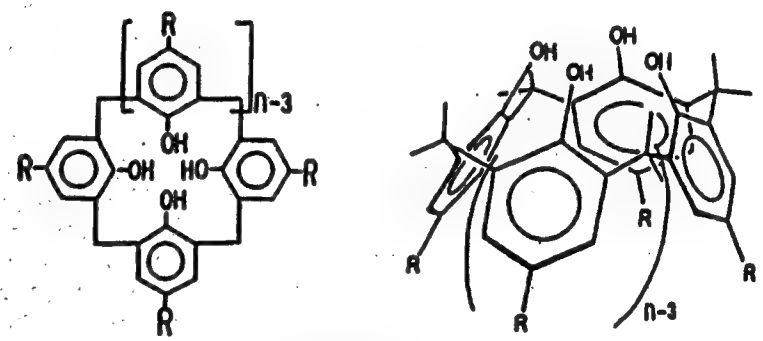

Calix[n]arene

In unmodified calix[4]arenes(1) cone conformers are the most stable because of intramolecular hydrogen-bonding interactions. In tetra-O-methylated calix[4] arene(2R), on the other hand, we could observe four conformers which exchange with each other in an NMR time-scale.[2,3] The relative stability is in the order of partial-cone (the most stable) > cone > 1,2-alternate > 1,3-alternate.

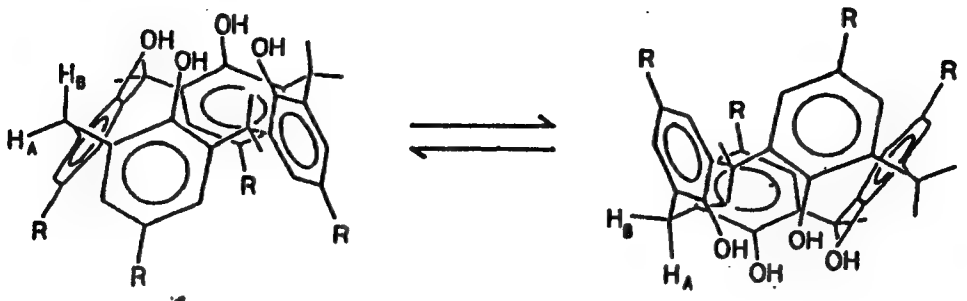

1

This order can be reasonably reproduced by MM3 calculations.[3] When O-substituent are bulkier than Et, the rotation no longer takes place. We can thus design novel ring-originating "chiral calix[4]arenes" by utilizing regioselective O-substitution and/or conformational isomerism.[4]

Table. Optically-Active Isomers Found in Tetra-O-Substituted Calix[4]arene

number of different substituents		cone	partial cone	1,2-alternate	1,3-alternate
1	AAAA				
2	AAAB				
	ABAB				
	AABB				
3	AABC				
	ABAC				
4	ABCD				

Metal-Ion Sensing: How Can We Recognize Metal Ions and Read-out the Binding Event?

It is known that calix[4]aryl esters (3R) show the high Na^+ selectivity. We synthesized several 3R derivatives which are useful in an ion-selective electrode system. Eventually, we found that 3Oct[5] shows the Na^+/K^+ selectivity higher than 10^3.[5] This is the first example that the artificial ionophore for Na^+ exceeds the selectivity higher than 10^3.

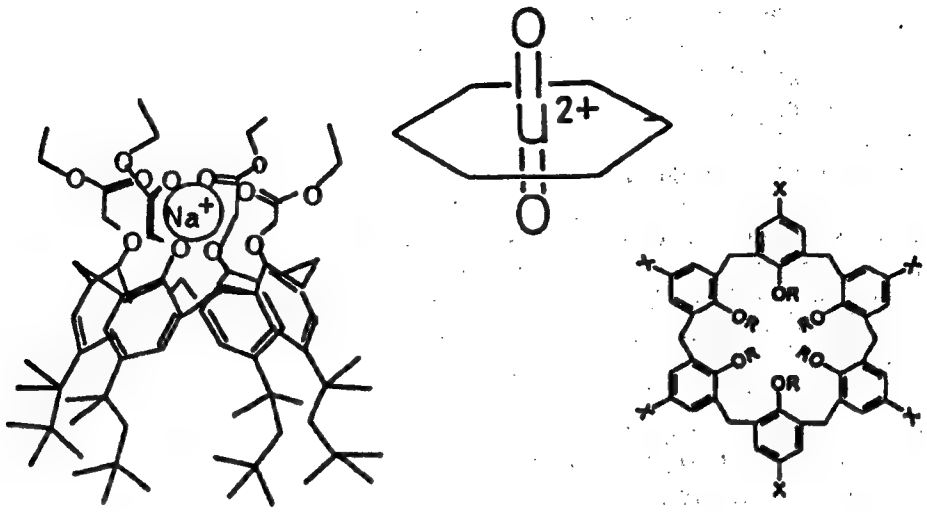

30ct[t]

4

Calixarenes-based ionophores are also useful for the selective-binding of rare-earth metal ions. X-ray crystallographic studies have established that UO_2^{2+} complexes adopt a hexacoordinate structure, which is quite different from the coordination structure of other metal ions. This suggests that a macrocyclic host molecule having a nearly coplanar arrangement of six ligand groups would serve as a specific ligand for UO_2^{2+}. We found that calix[6]arenes exactly satisfy this prerequisite. Compounds 4 showed $K_{ass} = 10^{18-19}$ M^{-1} and the selectivity $K_{uranyl}/K_{M+} > 10^{12}$.[6] Thus, compounds 4 are the best "super-uranophiles exploited so far.

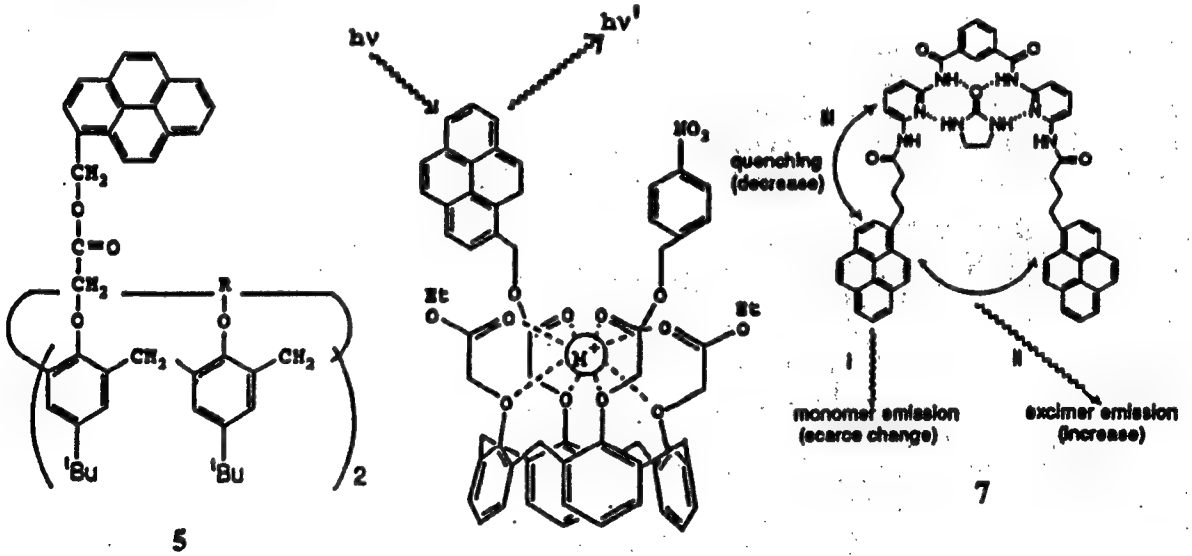

5

6

7

To sensitively read-out the metal-binding event by some spectroscopic method, we synthesized 5 and 6.[7] In vacant calix[4]aryl esters the carbonyl groups are turned outward whereas they are turned inward when the metal ion is bound into

the cavity. This induces a change in the relative spatial position of two fluorophores. In 5 we can observe a large decrease in excimer emission. In 6 we can observe a large increase in monomer emission. In 6 we can observe a large increase in monomer emission. This concept is applicable to molecular recognition as shown in 7.[8]

Molecular Inclusion: Hydrophobic Force Vs. Cation-π Interaction

Since calixarenes possess a cylindrical architecture similar to cyclodextrins, they are expected to include organic guest molecules. In the solid state they do include guest molecules, but the data related to solution complex have been very limited. We found that in an aqueous system, water-soluble calixarenes (8) form complexes with a variety of organic guests molecules.[9-11] Very interestingly, 8 includes the phenyl moiety of 9 at acidic pH whereas it includes the ammonium moiety of 9 at basic pH. This implies that at acidic pH the driving force for guest inclusion is "hydrophobic force" whereas at basic pH it is "cation–π interaction." We now consider that cation–π interactions should be more taken into account, which govern the molecular inclusion and the orientation of host-guest complexes. In fact, we have many data which can be reasonably explained on the basis of "cation–π–interaction."

Recognition in Molecular Assembly Systems

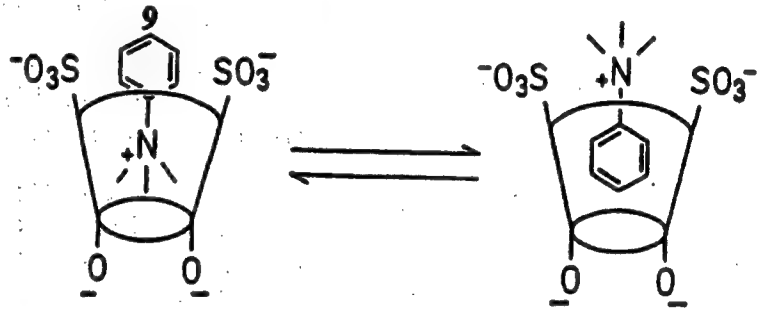

8

Compounds 10 have both H-bond donors (OH) and H-bond acceptors within a molecule. Interestingly, we found that they act as new gelators of various organic fluids.[12,13] Compounds 11 include liquid-crystal-forming azomethine units in a star-burst manner. Actually, they did not form the liquid crystal but showed the flow birefringence.[14] These systems are useful as a new class of molecular receptor in molecular assembly systems.

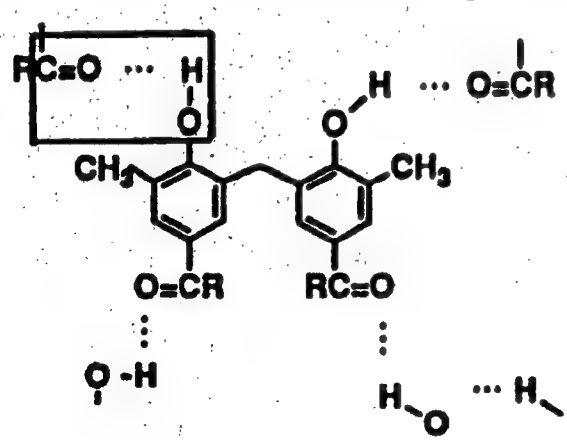

10

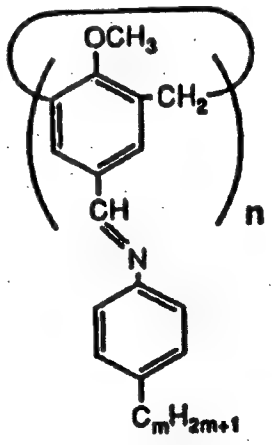

11

References

1. K. Araki, S.Shinkai, and T. Matsuda, *Chem. Lett.*, **1989**, 581.
2. K. Iwamoto, K. Araki, and S.Shinkai, *J. Org. Chem.*, **56**, 4955 (1991); Idem, *Tetrahedron*, **47**, 4325 (1991).
3. T. Harada, T. M. Rudzinski, and S. Shinkai, *J. Chem. Soc., Perkin Trans. 2*, in press.
4. S.Shinkai, T. Arimura, H. Kawabata, H. Murakami, and K. Iwamoto, *J. Chem. Soc., Perkin Trans. 1*, **1991**, 2429; K. Iwamoto, A. Yanagi, T. Arimura, T. Matsuda, and S. Shinkai, *Chem. Lett.*, **1990**, 1901.
5. T. Sakaki, T. Harada, and S. Shinkai, to be submitted.
6. S. Shinkai, H. Koreishi, K. Ueda, T. Arimura, and O. Manabe, *J. Am. Chem. Soc.*, **109**, 6371 (1987).
7. I. Aoki, H. Kawabata, K. Nakashima, and S. Shinkai, *J. Chem. Soc., Chem. Commun.*, **1991**, 1771; I. Aoki, T. Sakaki, and S. Shinkai, *ibid.*, **1992**, 730.
8. I. Aoki, T. Harada, T. Shinkai, Y. Kawahara, and S. Shinkai, *J. Chem. Soc., Chem. Commun.*, in press.
9. S. Shinkai, K. Araki, and O. Manabe, *J. Am. Chem. Soc.*, **110**, 7214 (1988).
10. S. Shinkai, K. Araki, T. Matsuda, N. Nishiyama, H. Ikeda, I. Takasu, and M. Iwamoto, *J. Am. Chem. Soc.*, **112**, 9053 (1990).
11. S. Shinkai, S. Mori, H. Koreishi, T. Tsubaki, and O. Manabe, *J. Am. Chem. Soc.*, **108**, 2409 (1986).
12. S. Shinkai, T. Nagasaki, K. Iwamoto, A. Ikeda, G.-X. He, T. Matsuda, and M. Iwamoto, *Bull. Chem. Soc. Jpn.*, **64**, 381 (1991).
13. M. Aoki, K. Murata, and S. Shinkai, *Chem. Lett.*, **1991**, 1715.
14. T. Komori and S. Shinkai, *Chem. Lett.*, **1992**, 901.

Laser Manipulation, Spectroscopy, Preparation in Molecular Systems

43070028D Fukuoka JRDC FUKUOKA PREFECTURE in English 25 Nov 92 pp 19-22

[Article by Hiroshi Masuhara, Microphotoconversion Project, ERATO Program, Research Development Corporation of Japan]

[Text] Small microspheres such as microcapsules, liquid droplets, polymer latex particles, and biological cell in solution diffuse under a Brownian motion. Polymers and molecular assemblies also move randomly in solution. To characterize a single microsphere/assembly and to induce chemical reactions in it, it is necessary to introduce a new method for selecting a microsphere/assembly and fixing it at a certain position under a microscope. This is recently achieved by a newly developed optical trapping technique utilizing a focused 1064 nm laser beam. The second UV laser pulse is additionally introduced for exciting a single trapped microsphere/assembly, and now its manipulation, picosecond spectroscopy, photochemical reaction, fabrication, and preparation are possible in solution.

Laser Manipulation

The conditions for laser trapping are summarized as follows: (1) spherical shape is favorable, (b) the refractive index of the sphere is larger than that of the surrounding medium, (c) an intense beam is needed, (d) the beam is focused with an objective lens of a large NA value, and (e) the sphere is transparent at the laser wavelength. Laser beam focused to a small microsphere under such conditions exerts an optical pressure, leading to trapping of the microsphere. As is shown in Fig. 1, the beams a and b, for example, are refracted at the surface of the particle. The momentum change upon refraction (Fig. 1-B) is transferred to the particle, namely, a force is exerted on the particle like F_a and F_b. The sum of these forces is directed to the focus of the objective lens and the particle is trapped at the focus point. The trapping force depends on laser intensity, particle size, refractive index, and optics, and exerted power of pN is enough for trapping the microsphere.

A more sophisticated way of manipulation was innovated by scanning the focus point with a computer-controlled set of galvano mirrors. The spot of the laser beam was respectively driven with high frequency, then particles were trapped along its locus. Viscous solvent was used as a medium to prevent quick escape of the particle from the trapping well, and an average power of the scanned laser beam is enough high to suppress the Brownian motion. It is worth noting

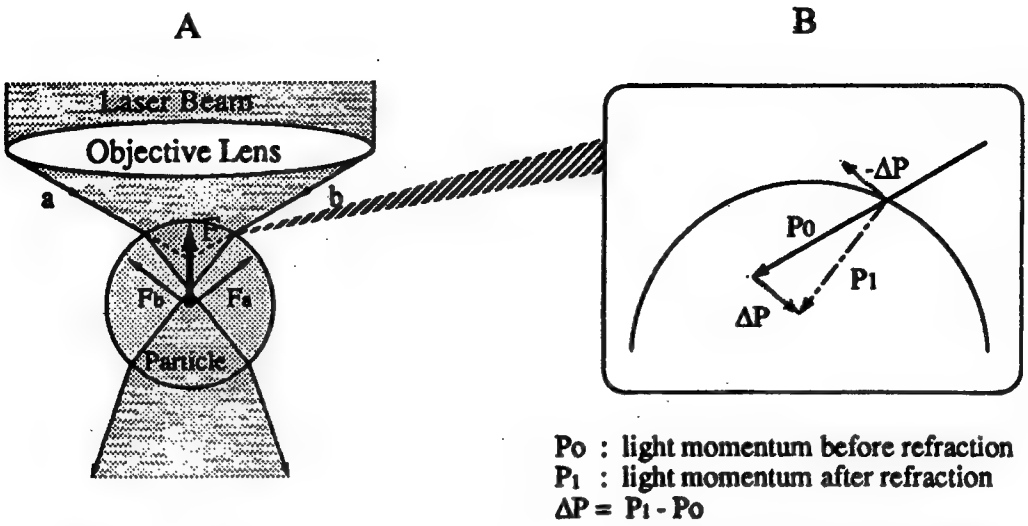

Figure 1. Force Exerted on a μm-Size Sphere in Laser Trapping

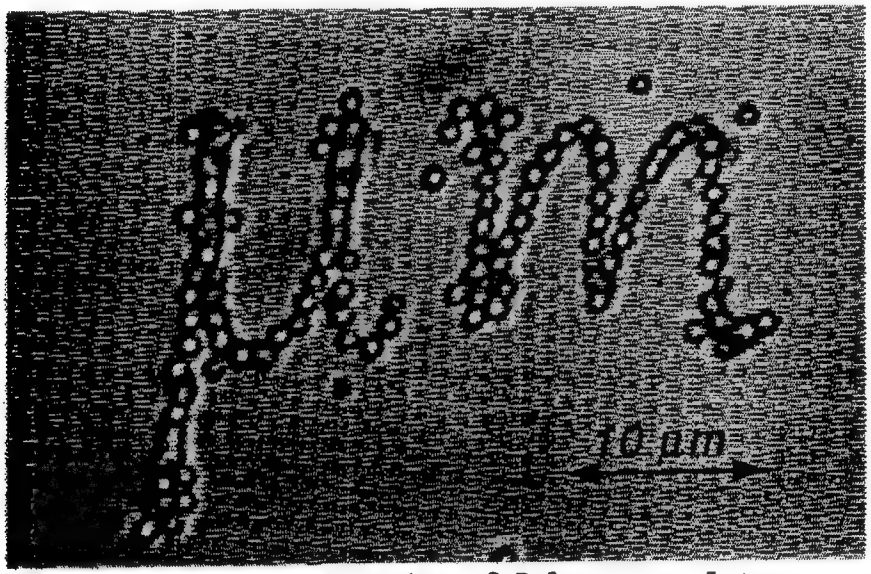

Figure 2. Spatial Patterning of Polystyrene Latex Particles (diameter ~ 1 μm) in Ethylene Glycol at Room Temperature
Total laser power ~145 mW, repetition rate = 13 Hz.

that various patterns such as letters, starts, and so on can be formed and transported by the laser scanning micromanipulation. One example is shown in Figure 2.

Picosecond Spectroscopy and Photochemistry

Characterization and analysis of a single microsphere in solution is performed by transient fluorescence and absorption spectroscopy. A space- and time-resolved spectroscopy is realized with a confocal laser scanning microscope and combined with the laser manipulation method. Subμm, ps, and nm are attained for spatial, temporal, and spectral resolutions, respectively. Pyrene

excimer formation dynamics is analyzed as a model in a single microcapsule and liquid droplet. It is discussed that photophysical and photochemical properties of microsphere/assembly can be revealed only by measuring the dynamics of individual particles.

Laser Fabrication

Increasing the excitation intensity, excited states are populated densely leading to laser ablation. One shot excitation of the trapped microsphere produced a small pinhole with the diameter of less than 1 μm, and the decomposed fragment was ejected into water. Excitation of the polymer latex particle with repetitive laser pulse resulted in a complete destruction. Since its spherical shape is broken, it cannot be trapped anyone and undergo Brownian diffusion.

A microcapsule containing toluene solution of pyrene in water was trapped and excited. A nanosecond 355 nm pulse was absorbed by pyrene, and photochemical and photothermal processes were initiated. The deformation, bubble formation, and destruction of the capsule were observed depending on the laser intensity, and the inner toluene solution was ejected to water. The ejected liquid was also trapped as a droplet by the trapping beam. It is possible to manipulate a single capsule, to fix it at a certain position, and to remove the inner liquid by laser ablation, and to modify chemically the minute surface area of various materials.

Laser Preparation

As an example of laser preparation of a microsphere/assembly, reversible microsphere formation/dissolution of poly(N-isopropylacrylamide) in water was studied by a focused 1064 nm laser beam. Its aqueous solution exhibits a phase transition at 31-32°C above which the polymer chains associate with each other to form water-insoluble polymeric particles owing to a large increase in hydrophobicity of the polymer. At room temperature the aqueous solution is a microparticle was produced almost instantaneously in the focal point of the laser beam. When the laser was turned off, the prepared microparticle disappeared quickly. Formation and dissolution of the microparticle was highly reversible for several cycles without any appreciable change in the equilibrium diameter of the particle.

The volume and density of the associated polymer chains increased refracting the laser beam, and the exerted power packed the chains further, accelerating the refraction. Thus the particle with smooth surface was formed, which can be ascribable to concerted effects of radiation force and local heating of H_2O by the 1064 nm laser beam. The prepared microparticle can be characterized by fluorescence spectroscopy, manipulated, and fabricated.

Conclusion

Manipulation, spectroscopy, and preparation of microspheres and molecular assemblies can be achieved in the small domains by utilizing lasers. In the near future the smaller size of a microsphere/assembly will be examined, and its structure and dynamics will be revealed by laser spectroscopy and photochemistry.

Artificial Supramolecular Receptors for Biologically Active Molecules at Air-Water Interface

43070028E Fukuoka JRDC FUKUOKA PREFECTURE in English 25 Nov 92 pp 27-30

[Article by Toyoki Kunitake, Supermolecules Project, JRDC, and Faculty of Engineering, Kyushu University]

[Text] **1. Introduction**

Molecular recognition is a key concept in many areas of chemistry. The use of multiple hydrogen bonding as a means of specific recognition is especially popular in recent years. This interest is derived from its analogy to molecular recognition in the biological system.

The previous host molecules have been effective only in organic solvents, due to deteriorating influences of water against the host-guest hydrogen bonding. However, sites of molecular recognition in the biological system are usually exposed to the aqueous phase. It is therefore desirable to develop artificial host systems that can recognize guest molecules in direct contact with bulk water.

Organized molecular assemblies on water are uniquely suited for this purpose. Their macroscopic and microscopic organizations are readily characterized by the conventional physicochemical method, and binding functional units can be placed in fixed spatial arrangements in exposure to the aqueous subphase.

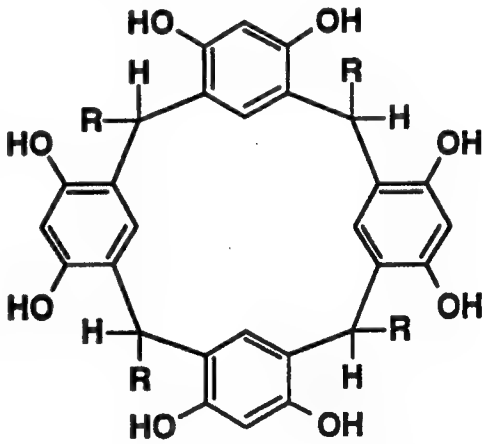

$R:(CH_2)_{10}CH_3$

1

2. Specific Binding of Sugars by Hydrogen Bonding[1]

Resorcinol-dodecanal cyclotetramer 1 forms a stable monolayer at the air-water interface. Molecular interactions of this monolayer with sugars and related water-soluble substances have been studied by combinations of potentiometric responses of monolayer modified SnO_2 electrodes, UV-visible, FT-IR, and

XPS spectroscopies of LB films, and surface pressure–area isotherms. Sugars and water-soluble polymers bearing hydrogen-bonding groups bind to this monolayer selectively, resulting in anodic potentiometric responses of the 1-modified electrode.

The affinity of sugars to monolayer 1 increases in the order: glucose < fucose, galactose, arabinose < xylose < ribose. This selectivity is different from that of sugar extraction into CCl_4 from the aqueous phase: ribose is bound to 1 effectively in both systems, while fucose, which is easily extracted into CCl_4, is less effective in the monolayer system. Galactose, which is complexed weakly in CCl_4, shows significant binding to the monolayer. Formation of sugar complexes which expose more hydroxyl groups and less lipophilic parts to water is preferred at the interface. Binding to the monolayer host is efficient owing to the high densities of host molecules aligned at the interface. The present results strongly indicate that the specificity of sugar binding is brought out by hydrogen bonding; the present of multiple hydroxyl groups and their fixed mutual arrangements in resorcinol cyclotetramer is required to obtain efficient sugar biding.

3. Convergent Binding Sites Formed by Kemp's Acid Derivatives[3]

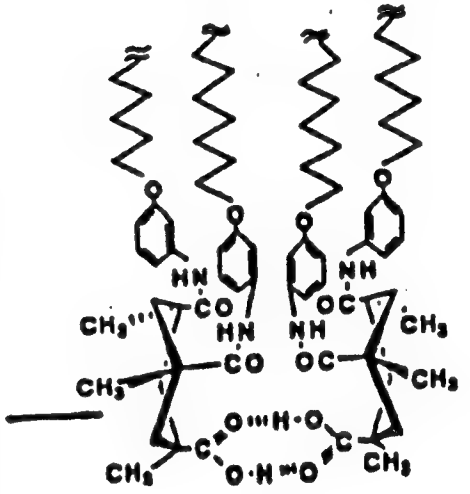

2

Long-chain derivatives of Kemp's acid form stable monolayers at the air–water interface, where the carboxylic acid groups produce the cyclic dimer species and serve as a molecular cleft for specific binding of nitrogen aromatics and amino acids. The structure of the long-chain substituent is crucial for forming the cyclic dimer. Substrates of complementary shape and functionality are bound to the cleft mainly by hydrogen bonding. Phthalazine forms a 1:2(substrate/amphiphile) complex, and its enhanced binding (binding constant, 30 M^{-1}) compared to those of quinoxaline, and pyridazine is ascribable to the proper location of nitrogen atoms within the molecule as well as smaller solubility in water. A more basic substrate, benzimidazole, is bound to the monolayer five times more strongly probably in a form of the 1:1 complex. The monolayer of octadecenoic acid is not an effective receptor, implying that the convergent carboxylic acids are the intrinsic element of the molecular recognition.

4. Binding of Phosphate-Bearing Substrates[3]

The guanidinium moiety is an important interaction unit for many biological receptors due to its unique combination of cationic and hydrogen-bonding properties. Amphiphile 3 forms a monolayer on pure water. The monolayer behavior is altered significantly by addition of 1 mM Na ATP and Na AMP. ATP causes a condensation of the π–A curve, whereas AMP makes the curve more expanded. The XPS data clearly establish that the substrate binding occurs very effectively through specific formation of the guanidinium–phosphate pair at the air–water interface.

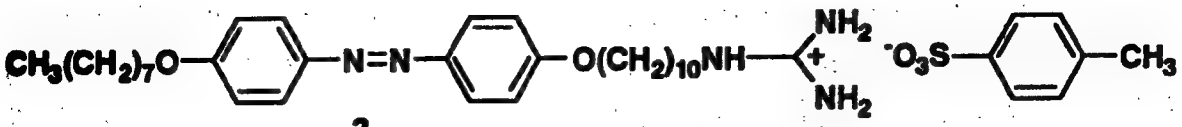

3

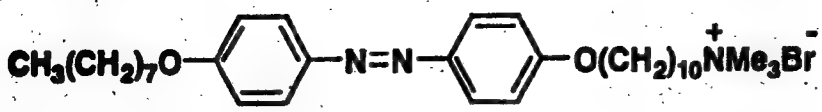

4

The hydrogen-bonding interaction must be responsible, in addition to the electrostatic interaction Supportive evidence for this presumption was obtained by ATP binding experiments against monolayer 4, which is the trimethylammonium counterpart of 3. A conceivable mode of binding is illustrated in the case of ATP in Figure 1.

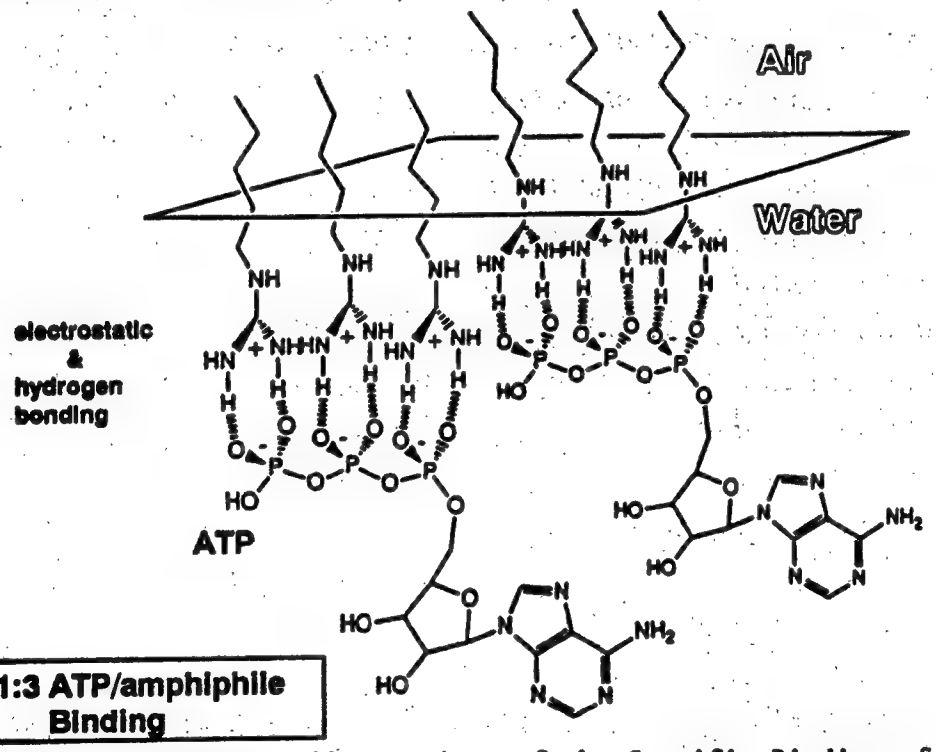

Figure 1. Schematic Illustrations of the Specific Binding of ATP to Guanidinium Monolayer at the Air-Water Interface

5. Guest Binding by Complementary Hydrogen Bonds[4-6]

A diaminotriazine amphiphile 5 forms a stable monolayer. Its surface pressure-area isotherm shows an expanded phase at 20.0±0.2°C. Thymidine and uridine dissolved in the aqueous subphase (0.01 M) only slightly expand the monolayer. The C:N:O ratio of an LB film from 0.01 M thymidine is (75.5±0.9):(14.1±0.6):(10.4±0.3)(%), and is close to ah computed atomic ratio of 1.1:1 for thymidine

to 5: i.e., C:N:O = 75.6:14.2:9.8. Similarly, the molar ratio of bound substrate was estimated as 1.1,1.1, 0.5, and 0.2 for 0.01 M urdine, thymine, and adenosine and 0.003 M adenine, respectively. Equimolar amounts of thymidine, uridine, and thymine are bound to the host monolayer at 0.01 M.

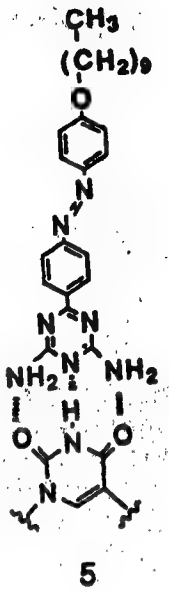

5

Therefore, thymidine, uridine, and thymine (substrates bearing the imide moiety) are bound to monolayer 5, in preference to adenosine and adenine. Complementary hydrogen bonds between the diaminotriazine unit and the imide moiety (Figure 2) apparently causes the selective binding. The association constants of thymidine and thymine with monolayer 5 are estimated to be $(2\pm1) \times 10^2 M^{-1}$, by assuming the Langmuir adsorption.

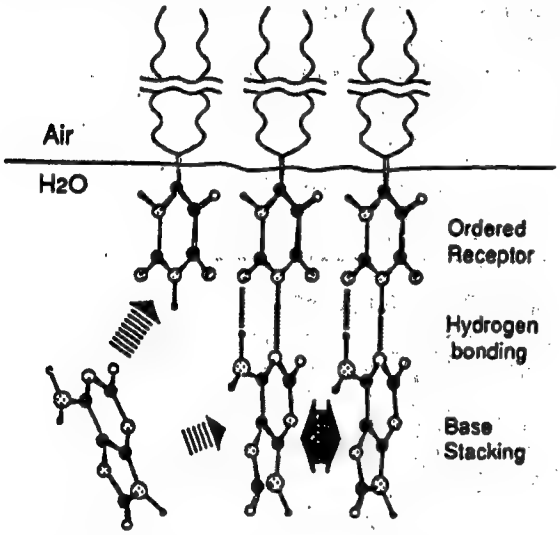

Figure 2. Cooperative Binding of Adenine to Orotonate Monolayer 6

These monolayers also display specific binding of barbituric acid and thiobarbituric acid via [as published]

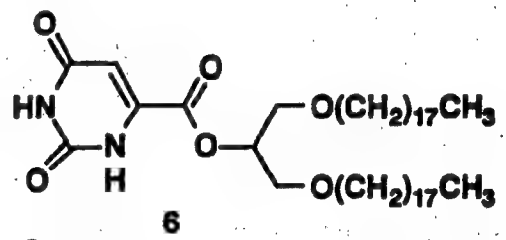

6

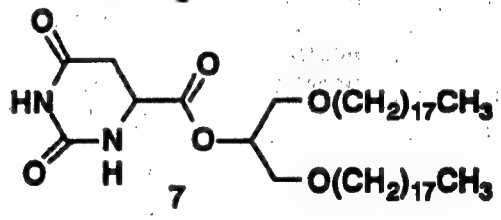

7

Double-chain derivatives of orotic acid 6 and hydroorotic acid 7 commonly contain cyclic imide (uracil-like and hydrouracil-like) structures that are complementary to adenine, but their electronic and steric structures are different. Amphiphiles 6 and 7 form stable monolayers on pure water with collapse pressure of 40-50 mN/m and limiting molecular areas of 0.4 nm^2/molecule. The collapse pressure of monolayer 6 decreases at adenine concentrations greater than 1 mM in the subphase; whereas the surface pressure-area (π-A) behavior of monolayer 7 is not affected by adenine. Addition of thymine in the subphase did not cause any change in π-A isotherms of the two monolayers. This monolayer behavior strongly suggests that only adenine is selectively bound to monolayer 6. Direct confirmation of substrate binding was subsequently conducted by FT-IR and XPS spectroscopies.

The selective binding of monolayer 6 with adenine but not with thymine is readily explained by assuming the Watson-Crik hydrogen bonding mechanism.

Another interesting feature is that monolayer 6, but not 7, binds adenine. The uracil ring in 6 is planar, but 7 assumes a nonplanar lactam (dihydrouacil) structure in preference to four kinds of less stable lactim tautomers. The lack of coplanarity in the interacting imide moiety would exert serious detrimental effects on complementary hydrogen bonding with adenine.

References

1. Kurihara, K., Ohto, K., Tanaka, Y., Aoyama, Y., and Kunitake, T., J. AM. CHEM. SOC., Vol 113, 1991, p 444.

2. Ikeura, Y., Kurihara, K., and Kunitake, T., J. AM.CHEM. SOC., Vol 113, 1991, p 7342.

3. Sasaki, D.Y., Kurihara, K., and Kunitake, T., J. AM.CHEM. SOC., Vol 113, 1991, p 9685.

4. Honda, Y., Kurihara, K., and Kunitake, T., CHEM. LETT., 1991, p 681.

5. Kurihara, K., Ohto, K., Honda, Y, and Kunitake, T., Vol 113, 1991, p 5078.

6. Kawahara, T., Kurihara, K., and Kunitake, T., CHEM. LETT., 1992, p 1839.

Understanding Cell Specificity, Carbohydrate-Carbohydrate Interaction Using Polysaccharide-Coated Liposome

43070028F Fukuoka JRDC FUKUOKA PREFECTURE in English 25 Nov 92 pp 37–42

[Article by Junzo Sunamoto, Kazunari Akiyoshi, Toshinori Sato, and Yukihisa Okumura, Department of Polymer Chemistry, Kyoto University]

[Text] **Introduction**

"*Supramolecular assembly*" is defined as a self-organized system constituted by various relatively weak and noncovalent bondings such as hydrogen-bonding, charge transfer interaction, hydrophobic interaction, and so forth. Such the supramolecular assemblies show unique properties or reactivities quite different from those of ordinary and small unimolecule. They sometimes provide novel function(s) that ordinary molecules can not perform. This is very common in nature, because most of living systems are based on the chemistry of supermolecules. For example, we are able to find the most completed example within a cell that is the smallest unit of life. In cell membranes, various membrane proteins associate with lipids and play an important role in intercellular communication, cell-cell adhesion, information transfer and mass transportation across the cell membrane.

During the past decade, we have extensively developed the coating of the surface of lipid monolayer [1,2], black lipid membrane [3], or liposome [4] with a hydrophobized polysaccharide [5] (Fig. 1) in order to mimic the structure and function of carbohydrates on cell surface. Especially, we have carried out basic investigations of intercellular communication, ligand-receptor interaction on cell surface, and receptor-mediated cell uptake by using an artificial cell liposome coated with an artificial cell wall; namely, a cell specific polysaccharide derivative, and developed missile (cell specific) drug delivery systems [6] and liposomal vaccines [7] in medicine and serum free cell culture in biotechnology [8].

In this paper, brief overview of the self-aggregation of hydrophobized polysaccharides in water, the coating of the outermost surface of liposomes with these hydrophobized polysaccharides, their cell recognizability, and specific carbohydrate-carbohydrate interaction will be made.

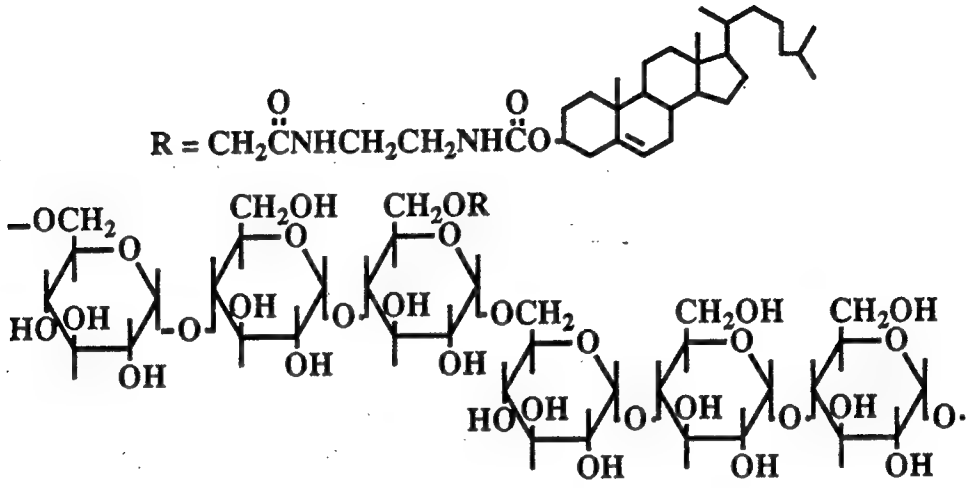

Fig. 1. An example of hydrophobized polysaccharide, CHP

1. Self-aggregation of hydrophobized polysaccharides [9].

A cholesterol-substituted pullulan derivative (coded as CHP) was synthesized by the reaction between pullulan (K. K. Hayashibara) and cholesteryl *N*-(6-isocyanatehexyl)carbamate, while a palmitoyl pullulan derivative (coded as OPP) also was synthesized by the similar method using palmitoyl chloride. Structures of the pullulan derivative is shown in Fig. 1. The abbreviation CHP-50-5.5, for example, refers to pullulan (MW 50,000) substituted with 5.5 cholesterol groups per 100 glucose units. ANS (magnesium 1-anilinonaphthalene-8-sulfonate) is a well known fluorescent probe to obtain information about microscopic polarity and/or viscosity of molecular assembly systems. The change in fluorescence intensity of ANS as a function of concentration of the pullulan derivative gave a straight line bent at a specific concentration of the polymer.

This concentration (the critical concentration) depends on the structure and the molecular weight of the parent polysaccharide and the substitution degree and the structure of hydrophobic substituents. In any event, the hydrophobized polysaccharides certainly formed polymer self-aggregates above this critical concentration. A higher substitution of the cholesterol moiety gave a lower critical concentration. The major driving force for the aggregation is therefore ascribed mainly to the hydrophobicity of the cholesterol moiety. The palmitoyl group was less effective than the cholesterol group in forming self-aggregates. The suspension of CHP self-aggregates was, for example, prepared by swelling the polymer in water for 12 hr at 60 °C followed by sonication using a probe type sonifier (TOMY UD-201) at 40 W and room temperature. The hydrodynamic diameter of the colloidal particles so obtained was determined by dynamic light scattering (DLS) to be approx. 27 nm. Static light scattering (SLS) measurement indicated that one CHP-aggregate is consisted of about 15 CHP molecules. Nanoparticles so obtained were extremely stable and no change in the particle size was observed at all even during a period longer than one month.

2. Adsorption of hydrophobized polysaccharides onto lipid monolayer [1,2] and black lipid membrane [3] surfaces.

The extent of adsorption of CHP and CHAp (cholesteryl amylopectin) at the air-water interface has been assessed from the surface pressure measurements at constant area. It was found that the molecular area of these polysaccharide molecules are 0.40 nm^2 and 0.19 nm^2, respectively. These small molecular area indicate that sugar moieties of the polysaccharide derivatives studied are completely immersed in the aqueous phase. From surface potential measurements which provided an additional information concerning interfacial orientation of these molecules, it was assumed that in the case of CHP cholesteryl groups are vertically oriented towards the interface, while in

the case of CHAp cholesteryl moieties are lying flat exposing lateral CH_3 groups to the interface. Surface pressure and surface potential isotherms of egg PC monolayers were shown to be greatly modified in the presence of hydrophobized polysaccharides in the aqueous subphase. The results reveal the ability of both polysaccharide derivatives to penetrate the lipid monolayer. This effect was found superior for CHAp, which interacts strongly with the lipid even at very high surface coverages. CHAp, however, has a surprisingly pronounced compensating effect on surface potential of egg–phosphatidylcholine monolayers.

3. Coating of outermost surface of liposome with hydrophobized polysaccharides [4].

Plant and bacterial cell membranes are covered with a cell wall of polysaccharides. The cell wall maintains the shape and stiffness of cytoplasm and protects the plasma membranes against various chemical and physicochemical stimuli. In order to make a liposome more mechanically stable, the liposomal surface was coated with a naturally occurring polysaccharide which bears a hydrophobic anchor such as a cholesterol or palmitoyl residue. The effect of a hydrophobic anchor on the coating efficiency of the liposomal membrane was studied from the viewpoints of the permeability of a polysaccharide-coated liposome and the membrane fluidity. Through these investigations, it was found that coating of the liposomal surface with cholesterol derivatives of the polysaccharides was much better for decreasing the membrane permeability than that with *O*-palmitoylpolysaccharide.

Saccharide determinants play an important role in biological recognition such as antigen-antibody interaction and cell-cell adhesion. Since 1982 we have been developing a methodology to achieve the receptor-mediated targeting in liposomal drug delivery system (DDS). Various pullulan derivatives, which have both cholesterol and another monosaccharide terminal such as hexosamines and 1-amino-hexoses, were synthesized and employed for coating liposome. The lectin-induced aggregation and the phagocyte uptakes of such polysaccharide-coated liposomes were effectively controlled by changing only the terminal sugar residue of polysaccharide derivatives. Liposomes which were coated with these cell specific polysaccharides were utilized in DDS for treatment of cancer and infectious diseases, in preparing potent

liposomal vaccines, in enhancement of immunopotentiation, and in establishment of complete serum free cell culture system.

4. Study of carbohydrate-carbohydrate interaction using aqueous two phase system.

When two different, but basically missible each other, aqueous polymer solutions were combined, the two solutions separate into two different phases at a certain concentration. This is a well known phenomenum called the *"aqueous two phase system"*. Especially, the two phase system of polyethyleneglycol (PEG) and dextran (DEX) is physicochemically well characterized and the PEG solution separates towards the top phase while the DEX solution moves towards the bottom phase. This system has been utilized for separation and purification of proteins, enzymes, or cells [10]. When liposomes are further added to this aqueous two phase system, the liposome is almost quantatively rejected from both phases and locates at the interface. When the liposome was coated by a hydrophobized polysaccharide, however, the polysaccharide-coated liposome is somewhat partitioned to the bottom phase of the polysaccharide solution due to the chemical structure of the saccharide moiety of the liposomal surface. A system such as 4 % PEG(200)-8 % DEX(400) or 4 % PEG(200)-8 % Pullulan(450) was well separated by centrifugation at room temperature and 2000 $\times g$ for 20 min. Multi lamellar liposome (MLV) prepared from DPPC-cholesterol (3 : 1 by mol) was coated with CHP-50-2.0 or CHD-50-2.0. The partition of the polysaccharide-coated liposomes in the aqueous two phase system was flurometrically studied using the liposome which carries a water insoluble fluorescent probe, DPH (1,6-diphenyl-1,3,5-hexatriene). As the result, the strength of the carbohydrate-carbohydrate interaction in water was the following sequence of DEX-DEX >> Pullulan-Pullulan > DEX-Pullulan. Using exactly the same methodology, interactions in water between other mono and disaccharides and polysaccharides were investigated.

Acknowledgement

This research was financially supported by Grants-in-Aid for Scientific Research from the Ministry of Education, Asahi Grass Foundation, Mochida Memorial Foundation. We gratefully acknowledge the collaboration of Professors Kohei Hara, Nobuko Ishii, Tohru Segawa, and Hiroshi Shiku and their research groups in School of Medicine, Nagasaki University, and the dedicated contributions of coworkers whose names appear in the references.

References

[1] The Effect of Polysaccharide Adsorption on Surface Potential of Phospholipid Monolayers Spread at water-Air Interface, Adam Baszkin, Veronique Rosilio, F. Puisieux, G. Albrecht, and J. Sunamoto, *Chem. Lett.*, 299-302 (1990).

[2] Cholesteryl-Pullulan and Cholesteryl-Amylopectin Interactions with Egg Phosphatidylcholine Monolayers, A. Baszkin, V. Rosilio, G. Albrecht, and J. Sunamoto, *J. Coll. Int. Sci.*, **145**, 502-511 (1991).

[3] Improved Stability of Black Lipid Membranes by Coating with Polysaccharide Derivatives Bearing Hydrophobic Anchor Groups, J. Moellerfeld, W. Prass, H. Ringsdorf, H. Hamasaki, and J. Sunamoto, *Biochim. Biophys. Acta*, **857**, 265-270 (1986).

[4] Naturally Occurring Polysaccharide Derivatives Which Behave as an Artificial Cell Wall on Artificial Cell Liposomes, J. Sunamoto, T. Sato, T. Taguchi, and H. Hamazaki, *Macromolecules*, (1992) in press.

[5] Physicochemical Characterization of Cholesterol-Bearing Polysaccharides in Solution, K. Akiyoshi and j. Sunamoto, in "Organized Solutions Surfactants in Science and Technology", ed. by S. E. Friberg and B. Lindman, Marcel Dekker, Inc., 290-304 (1992).

[6] Site Specific Liposomes Coated with Polysaccharides, T. Sato and J. Sunamoto, in Liposome Technology, 2nd Ed., vol. III, ed. by G. Gregoriadis, CRC Press, (1992).

[7] Direct Transfer of Tumor Surface Antigen-Presenting Protein (TSAP) from Tumor Cell to Liposome for Making Liposomal Vaccine, J. Sunamoto, T. Noguchi, T. Sato, K. Akiyoshi, R. Shibata, E. Nakayama, and H. Shiku, *J. Controlled Release*, **20**, 143-154 (1992).

[8] Recent Topics of Liposomes in Medicine and Biotechnology, T. Sato and J. Sunamoto, in "Progress in Lipid Research, ed. by R. T. Holman, H. Sprecher, and J. L. Harwood, Pergamon Press, (1992).

[9] Self-aggregates of Hydrophobic Polysaccharide Derivatives, K. Akiyoshi, S. Yamaguchi, and J. Sunamoto, *Chem. Lett.*, 1263-1266 (1991).

[10] P. A. Albertsson, "Partition of Cell Particles and Macromolecules", 3rd ed., Wiley & Sons, New York (1986).

Two-Dimensional Crystallization of Proteins, Colloidal Particles

43070028G Fukuoka JRDC FUKUOKA PREFECTURE in English 25 Nov 92 pp 43-47

[Article by Kuniaki Nagayama, Protein Array Project, ERATO, JRDC]

[Text] **Abstract**

We report a novel type of two-dimensional (2D) crystal of proteins and colloidal particles. This 2D crystal is fabricated inside a thin film of protein solutions or monodisperse colloidal suspensions on a flat surface of solids or liquids. The significance of the 2D crystallization we develop is its active nature governed by controllable forces and flows, opposed to the diffusion mechanism in the conventional crystallization. With this active mechanism a single domain of hexagonally packed 2D crystals can grow within a short period, from several seconds up to a few minutes depending on the conditions controlled.

INTRODUCTION

Throughout the long process of Earth's evolution life has changed from relatively simple to highly sophisticated organisms. This sophistication relies on a simple strategy, "assembly". The information underlying such assembly is completely contained in the sequences of DNA, which guide the production of proteins from amino acids and regulate a "biological hierarchy", from single molecules to sophisticated supramolecules. Human technology has not yet been able to utilize proteins with such sophisticated forms because of the lack of knowledge of the assembly principle. To appreciate the tremendous capability of proteins the Protein Array Project [1] attempts to assemble the protein in a two-dimensional (2D) manner. The strategy adopted is to fabricate a 2D protein array with sophisticated crystal definition - molecular alignment and crystal form.

The process of 2D arraying is governed by various physicochemical factors, ranging from the molecular assembling in the initial stage to the molecular orientation adjustment in the final stage. The governing factors for the assembling are usually long-range attractive forces as observed in non-specific colloidal interactions. When proteins are isolated from each other by the inter-molecular distances of more than their own sizes, they behave simply as colloidal particles in a classical way exhibiting non-specific short- and long-range interactions. We are, therefore, interested in the assembly process. Since the assembling process of proteins and colloidal fine particles can thus be treated within the same theoretical framework, the assembling process in the 2D crystallization is emphasized in this report.

ASSEMBLING PRINCIPLE IN BIOLOGICAL SUPRAMOLECULES

As observed in life, component proteins automatically gather to complete their assembly resulting in the final forms, supramolecules such as ribosome and nucleosome. This self-assembly can be devided to two processes: the diffusion-limited aggregation (the random assembly) of individual protein molecules (Fig. 1), and the molecular orientation adjustment (specific interactions) due to the mutual recognition among the assembled proteins. The assembling usually occurs in a dispersion state in the living cell. Due to the limited cell volume (~1μm duameter) the assembly does not become a bottleneck of the supramolecular formation. This biological assembly framework is, however, inadequate for the array engineering of the scale much larger than the living cell because of the slow and uncontrollable mechanisms.

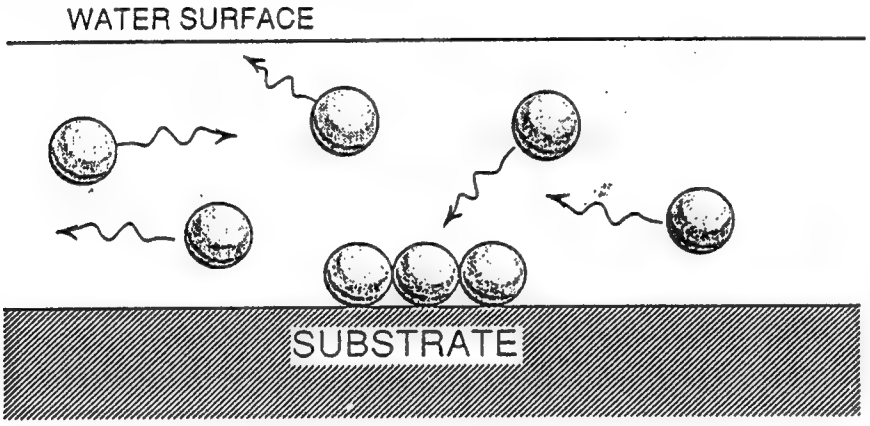

Fig.1. Particles assembly by the diffusion-limited aggregation in dispersions.

ASSEMBLING PRINCIPLES IN PARTICLE ARRAYS

In contrast with the supramolecules in dispersions, particle arrays grow on a substrate surface in a 2D form. The choice of an appropriate supporting surface is then important for the fabrication of highly ordered protein monolayers. In biosystems protein 2D crystals are often embedded in biological membranes, such as cell membranes and liposomes. The assembling inside the membranes again relies on the diffusion process. To replace the bilayer membranes by artificial substrates various kinds of interfaces such as water/air [2] and lipid/water/air [3] have been adopted. But, there is the same problem in these surfaces as described above (Fig. 1), the diffusion-limited assembly. Our recent innovation for the protein 2D crystallization using mercury has solved this problem. The technological breakthrough is the use of liquid thin films on the mercury surface. The additional consequence of this constraint

is the directional particle motion forced by the water flow that accelerates the crystal growth and facilitates making a large domain of 2D crystals in a short period. The waterflow speed and, therefore, the crystal growth speed is controllable by adjusting the evaporation rate and the thin film thickness.

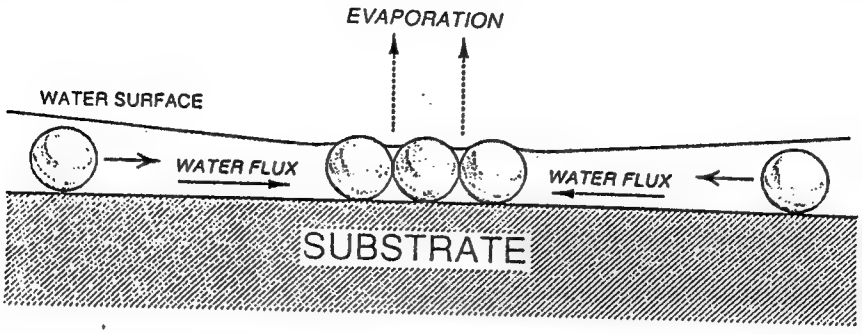

Fig.2. Particle assembly by waterflow in a liquid thin film (the flow-directed assembly).

2D COLLOIDAL CRYSTALS

With use of various sizes of polystyrene particles ranging from 50 nm to 2 μm, a unique method has recently been devised in our project. The significance of this method is the rapid growth of crystals and well ordered crystal arrays (Fig.2). The new assembly process is interpreted as follows [5]. As the water evaporates from the suspension, its thickness decreases with time (particles in the Brownian motion, Fig. 3a). The center of the concave meniscus first approaches the substrate resulting in a plane-parallel thin film. When this film becomes thinner than the particle diameter, an ordered 2D-domain forms due to the attractive immersion forces[6]. This domain is a nucleus inducing an ordered monolayer array. The array area increases with time (crystal growth, Fig. 3b). These new participants are conveyed according to the lateral water flow, which compensates the water evaporated at the nucleus[5]. After drying, a hexagonal 2D crystal remains on the substrate as shown in Fig. 3c.

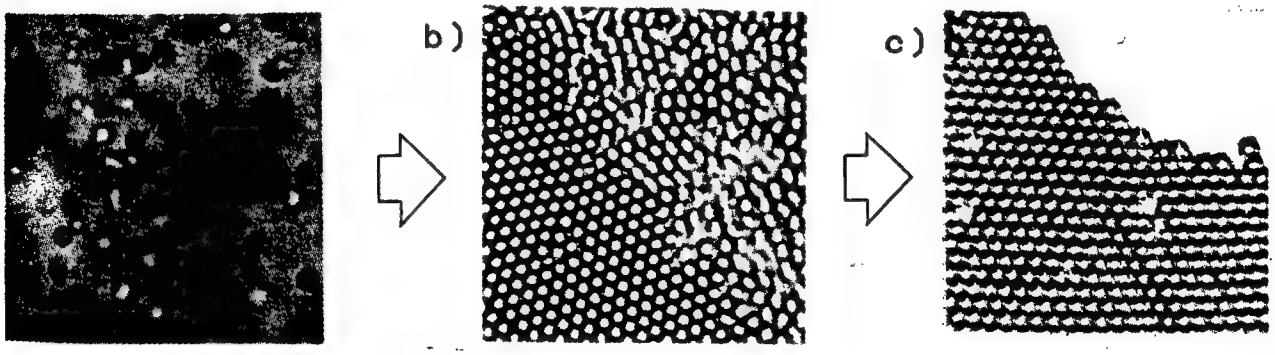

Fig.3 2D crystallization of colloidal particles (0.8 μm polystyrene latex particles) by the flow-directed assembly.

2D PROTEIN CRYSTALS

In order to obtain a clean and flat surface with high surface-energy enough to spread protein water solutions, we chose mercury as the substrate on which protein 2D crystals can be developed. An electron micrograph of this crystal is shown in Fig. 2, together with that obtained with random assembly method. With the mercury method the quality of lattice ordering is drastically improved (Fig.4). The schematics at the bottom clearly illustrate the essential advance due to replacing the conventional water surface by the thin liquid film. In addition, the crystallization is completed within a few seconds, thousand fold faster than the conventional method. Until now more than a dozen different proteins and protein complexes were crystallized using the mercury method, and one-third of the samples have appeared to be well ordered arrays. These include water-soluble proteins, ferritin[7], the water-soluble part of the H^+-ATPase from thermophilic bacterium, a membrane protein, bacterial hookbasal body complex (LP-ring)[8], and chaperonin from E. coli [9].

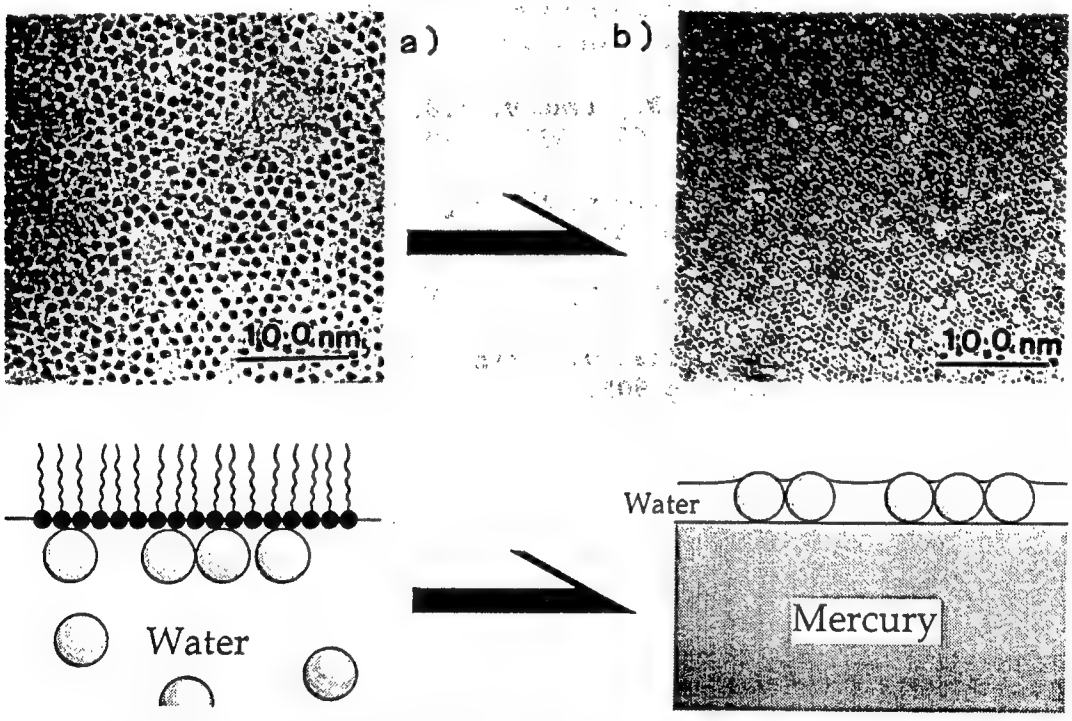

Fig. 4 2D crystallization of protein molecules (ferritin, Mw≅400kDa) by the random assembly (a) and the flow-directed assembly (b).

Acknowledgement:

This work is financially supported to its full extent by the Research & Development Cooperation of Japan. I thank the collaborators in the Protein Array Project, Dr. S. Ebina, Dr. P. Kralchevsky, Dr. I. Ivanov, Dr. C. Dushkin, Dr. N. Denkov, Dr. S. Endo and Dr. H. Yoshimura, and Dr. M. Matsumoto of Kyoto University for this work.

References

1. Nagayama, K., NANOBIOLOGY, Vol 1, 1992, p 25.

2. Pieranski, P. PHYS. REV. LETT., Vol 45, 1980, p 569.

3. Fromherz, P., NATURE, Vol 231, 1971, p 267.

4. Yoshimura, H., Matsumoto, M., Endo, S., and Nagayama, K., ULTRAMICROSCOPY, Vol 32, 1990, p 265.

5. Denkov, N.D., Velev, O.B., Kralchevskiy, P.A., Ivanov, I.B., Yoshimura, H., and Nagayama, K., Langmuir, in press.

6. Kralchevsky, P.A., Paunov, V.N., Ivanov, I.B., and Nagayama, K., J. COLL. INTERFACE SCI., Vol 151, 1992, p 79.

7. Yoshimura, H., Endo, S., Matsumoto, M., Nagayama, K., and Kagawa, Y., J. BIOCHEM., Vol 106, 1989, p 958.

8. Akiba, T., Yoshimura, H., Namba, K., SCIENCE, Vol 252, 1991, p 1544.

9. Ishii, N., Taguchi, H., Yoshida, M., Yoshimura, H., and Nagayama, K., J. BIOCHEM., Vol 110, 1991, p 905.

Nano-Manipulation of Biomolecular Motor

43070028H Fukuoka JRDC FUKUOKA PREFECTURE in English 25 Nov 92 pp 55-56

[Article by Toshio Yanagida, professor, Department of Biophysical Engineering, Osaka University, director, Biomotron Project, ERATO, JRDC]

[Text] We have developed a new system for measuring the force produced by a small number (1-100) of myosin molecules interacting with a single actin filament *in vitro*. The technique can resolve forces less than a piconewton on the submillisecond time scale and thus detect fluctuations of force due to the individual molecular events. Development of this new system followed the design of techniques for force measurement *in vitro* motility assay by manipulating single actin filaments attached to glass microneedles under a fluorescence microscope.

Analysis of force fluctuations (noise) is a very powerful approach toward determining kinetic characteristics of individual myosin heads interacting with actin, especially when the number of interactions is small as in the present conditions. Under isometric conditions, we have observed large force fluctuations similar to membrane current fluctuations due to channel gating in electrophysiological systems with small numbers of channels.

The force fluctuations in the isometric condition are consistent with models incorporating stochastic and independent molecular events. Both a simplified, two state, ON-OFF model and the Huxley (1957) model simulate the amplitude and frequency spectrum of the observed cross-bridge noise. Using these models we determined the ON and OFF rates and the force generated by single myosin heads. The data are compatible with one fundamental mechanical interaction for each ATPase cycle.

On the other hand, when the actin filaments slide at velocities greater than ~1 μm/s, fluctuations of force are much smaller. The data analysis indicates that myosin produces an almost constant force for greater than 90% of the ATPase cycle time. This result indicates that during siding, for each ATPase cycle there are many force-generating mechanical interactions between actin and myosin.

In conclusion, a new conceptual framework is needed to explain chemo-mechanical coupling in actomyosin motility. We propose that when work is done at higher velocity, the myosin head utilizes directly the free energy made available by the hydrolysis of a single ATP molecule for many working strokes. Alternatively, the energy could be efficiently transferred via actin to multiple myosin heads, to generate multiple working strokes.

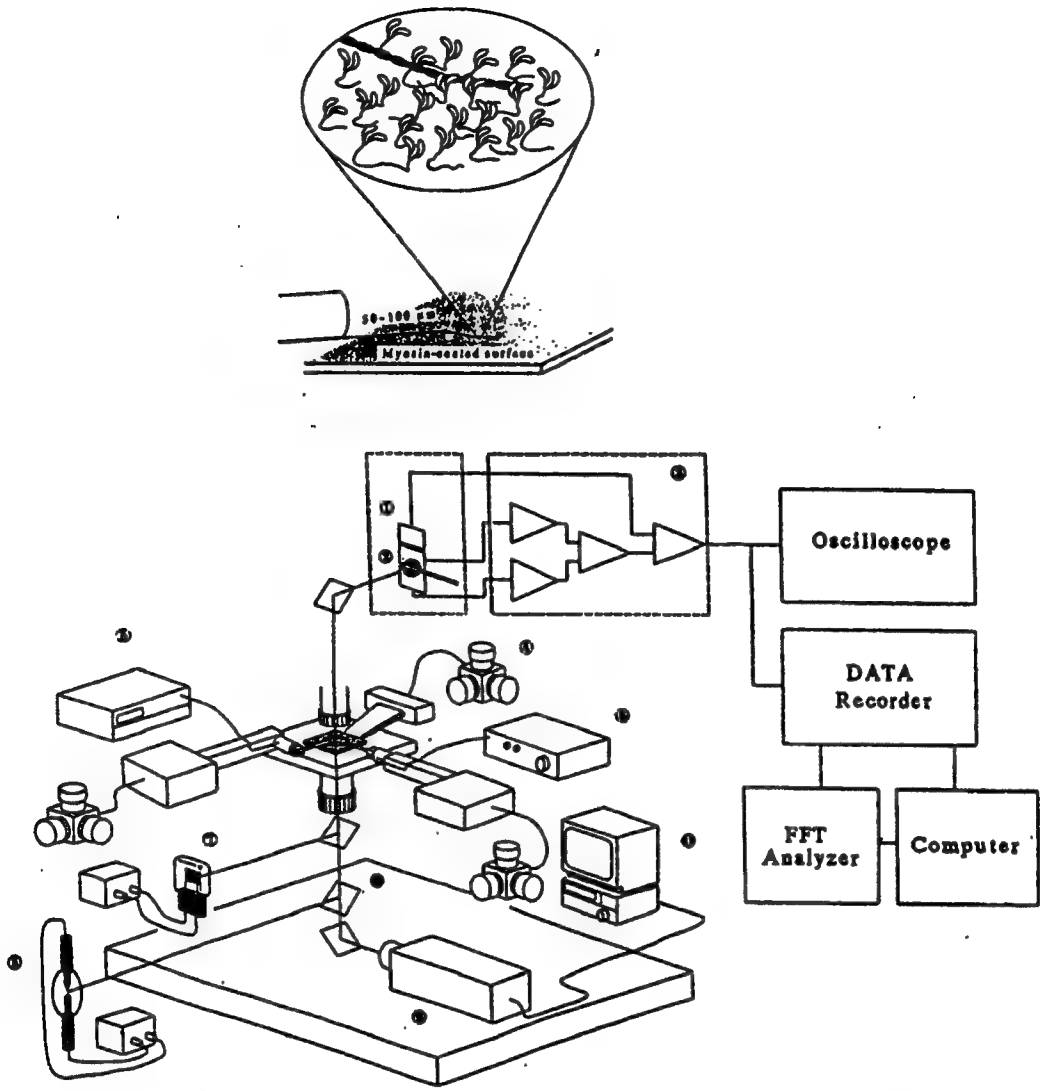

Schematic Diagram of Ultrahigh-Resolution Force Measurement System

The setup was built on an inverted fluorescence microscope (Olympus, IMT-2), modified to minimize mechanical vibrations and drift, and set on a vibration-free table (1, Heltz, HG-107LM). Fluorescence of the labeled actin filament was excited by 540 nm light from an ultrahigh-pressure mercury lamp (2) and a x100 oil immersion objective lens (Zeiss Neofluoar, NA 1.3). The fluorescent image of the filament was displayed on a TV monitor (3) by a high-sensitivity SIT camera (Hamama tsu-Photonics, C 2741) (4). The microneedle catching the actin filament was manipulated by a fine micromanipulator (Narishige, MR-88) (5) and a piezo-actuator (CTC, CTC-6094-5) (6). The displacement of the needle was measured as follows. The nickel particle was illuminated with 650-900 nm light from a highly stabilized halogen lamp (7) with <0.2% ripple of light intensity. The image of the nickel particle was projected onto a pair of photodiodes(Hamamatsu-Photonics, S2545) (8) through an objective lens (Olympus, ULWD CDPlan x 40) with a long working distance of 5 mm. The photodiode outputs, converted into voltage by I-V converters, were subtracted, referred to the incident light intensity by a divider circuit (Analog devices, AD-515) (9), and recorded on tape by a digital data recorder (TEAC, Rd-1010T). The differential signal was analyzed off-line by a fast Fourier transform (FFT) analyzer (Advantest, R9211A) and a computer (NEC, PC-9801).

References

1. Yanagida, T., Nakase, M., Nishiyama, K., and Oosawa, F., "Direct Observation of Motion of Single F-Actin Filaments in the Presence of Myosin," NATURE, Vol 307, 1984, pp 58–60.

2. Yanagida, T., Arata, T., and Oosawa, F., "Sliding Distance of Actin Filament Induced by a Myosin Crossbridge During One ATP Hydrolysis-Cycle," NATURE, Vol 316, 1985, pp 366–369.

3. Harada, Y., Noguchi, A., Kishino, A., and Yanagida, T., "Sliding Movement of Single Actin Filaments on One-Headed Myosin Filaments," NATURE, Vol 326, 1987, pp 805–808.

4. Kishino, A. and Yanagida, T., "Force Measurements of Micromanipulation of a Single Actin Filament by Glass Needles," NATURE, Vol 334, 1988, pp 74–76.

5. Ishijima, A., Doi, T., Sakurada, K., and Yanagida, T., "Sub-piconewton Force Fluctuations of Actomyosin *In Vitro*," NATURE, Vol 352, 1991, pp 301–306.

Formation of Bio-Supramolecules Beyond Self-Assembly: Bacterial Flagella

43070028I Fukuoka JRDC FUKUOKA PREFECTURE in English 25 Nov 92 pp 57-61

[Article by Hirokazu Hotani, Department of Biosciences, Teikyo University]

[Text] **Supramolecules: Assemblies of Biomolecules**

Biological organisms effectively perform highly sophisticated functions such as self-replication, energy conversion, information processing. Unit elements which perform these intricate functions are thought to be assemblies of biological molecules. Biomolecules such as proteins, nucleic acids or lipids assemble into a variety of cellular organelles by self-organization processes. And, they play key roles in a living cell. These assemblies are often called supramolecules. The supramolecules possess highly sophisticated characteristics as follows.

1. Each supramolecule has its own specific function, for instance, transport of chemical substances, synthesis of biological molecules, conversion of chemical energy to mechanical one and so on.
2. Supramolecules are built from constituent molecules by self assembly manner, without using any template, energy, or reaction catalyzer.
3. They transform their structure in response to environmental change so that they alter their characteristics to adapt to new circumstances.

The study on supramolecules will provide fundamental basis for the development of intelligent molecular machines which possess unique characteristics and functions such as self-organization, selective transport of specific substances, information processing in a thermally fluctuating environment, self-adjustment to environment and so on. These intelligent supramolecules are expected to open a novel field of "nanotechnology" other than microtechnology. We will discuss on assembly mechanism and transformation of bacterial flagella as a typical example of the supramolecules. This study has been done in Hotani Molecular Dynamic Assembly Project, ERATO Program, JRDC.

Flagellar Structure and Transformation

Bacterial flagellum, the organelles of locomotion, is a helical filament about 20 nm in diameter and around 10 mm long. Electron microscopic studies have shown that it is a cylindrical structure composed of a regular helical array of subunit protein,flagellin. Bacteria swim in a liquid by means of flagella which rotate like screw of a boat. Torque necessary for the rotation is generated at the basal structure of flagellum, which is composed of disk-like rings and a rod, and therefore is called a flagellar motor.

A helical flagellar bundle on a swimming bacterial cell often changed into another helical form. This polymorphic nature of bacterial flagella is remarkably interesting characteristics. Isolated flagellar filaments also display several kinds of discrete helical structures or straight structure in response to environmental changes. Interconversion among these structures have been induced in various ways, for instance, by changes in pH, ionic strength, concentrations of alcohols and sugars, temperature or by an abrupt change in direction of the torque.

Understanding how these polymorphic transitions occur at the molecular level will give us a deep insight into dynamic properties of supramolecules in general. For this purpose, We determined the tree dimensional molecular structure of the flagella by using X-ray fiber diffraction method. At first, a method to achieve a sufficient orientation of flagellar filaments in high density was developed using superconductive magnets. We have analyzed X-ray diffraction patterns from oriented sols of two types (L and R) of straight flagellar filaments. These two types of filaments are thought to be built up of subunits in either one of two distinct conformations which coexist in a regular array in the helical filaments.

It was revealed that 11-fold longitudinal helical array of subunits is tiled 3 to the left in L-type and 7 to the right in R-type. Longitudinal distances between subunits are 52.4 A in L-type and 51,6 A in R-type, and thus only 0.8 A difference, is responsible for regulating the plymorphic transition of flagellar filaments.

Molecular arrangement in in a flagellum is very efficient to obtain driving force in fluid. There is a functional allocation with domain structures in a subunit protein. A central hole exists for the transportation of flagellins through it.

Formation of Flagella

Bacterial flagellum is composed of three portions; flagellar filament, hook and flagellar motor. The main portion of helical shape is a polymer of single kind of protein subunits, flagellins. The flagellar filament itself has been reconstituted from monomeric flagellins by a self assembly process. The self-assembly way, however, is not enough sophisticated to construct whole structure of flagella. It requires the aid of connecting proteins, capping structure at the flagellar tip, transport of flagellin through channel and formation of binding domain on flagellin molecule.

Knowing which domains of the monomer correspond to which parts of the amino acid sequence, we now know the center part of the primary sequence forms a relatively large domain located outside of the filament and is exposed to the environment. Both terminal regions are conserved and form a relatively small domain at the core of the filament, determining the shape of this assembly independent of the other domain. These regions are partially unfolded and flexible in monomers, prohibiting monomers from spontaneously polymerizing into filament until they encounter the specific structure at the distal end of the flagellar filament. This understanding has allowed the automatic control of self-formation functions in both time and space.

Monomers are synthesized in the cell body, transported to the distal end of the flagellum and polymerized there. We have observed a hole of 6 nm in diameter at the center of the filament that is large enough to be a channel for flagellin export. Therefore, it is quite likely that flagellin monomers are transported though the central channel to the distal end and added onto the very end of the filament, upon which both terminal regions of the molecule become well folded, forming alpha-helical bundles with their axes parallel to the filament axis.

To join the flagellar filament portion and the hook, two kinds of connecting proteins (Hap1 and Hap2) are involved. The filament is rigid structure like as a steel screw, whereas hook is very flexible one like as a rubber tube. It seems general strategy to use connecting proteins for construction of the supramolecules which are composed of parts possessing remarkably different properties.

To understand how the flagella filament grows *in vivo*, we supplemented a cap deficient mutants with purified cap protein in the growth medium. The mutants then grew flagellar filaments and became motile. The purified cap protein assembled into a pentagonal star shaped structure with a diameter of about 10 nm. The turnover of the cap structure is not necessary for flagellar growth. consequently, flagellin must be incorporated directly underneath the cap structure.

Characteristcs of Biosupramolecules

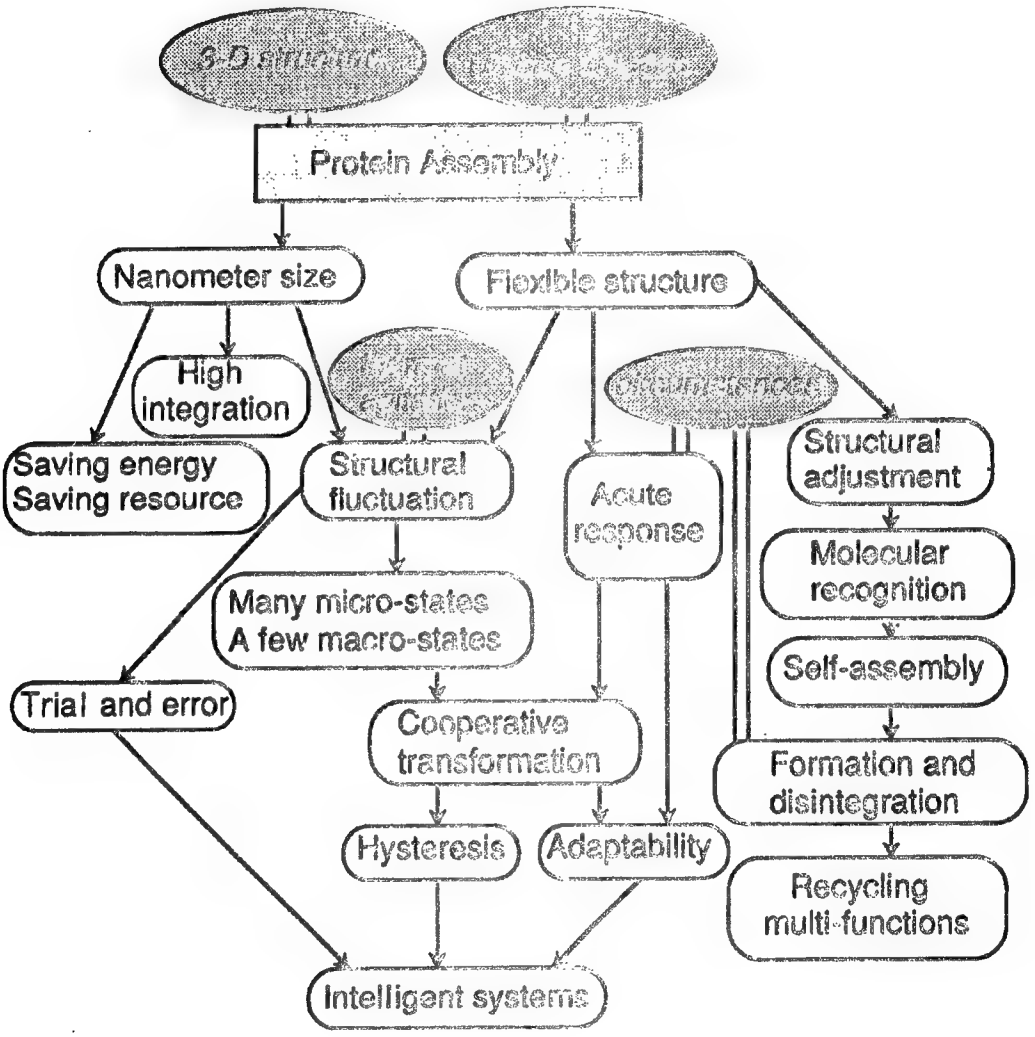

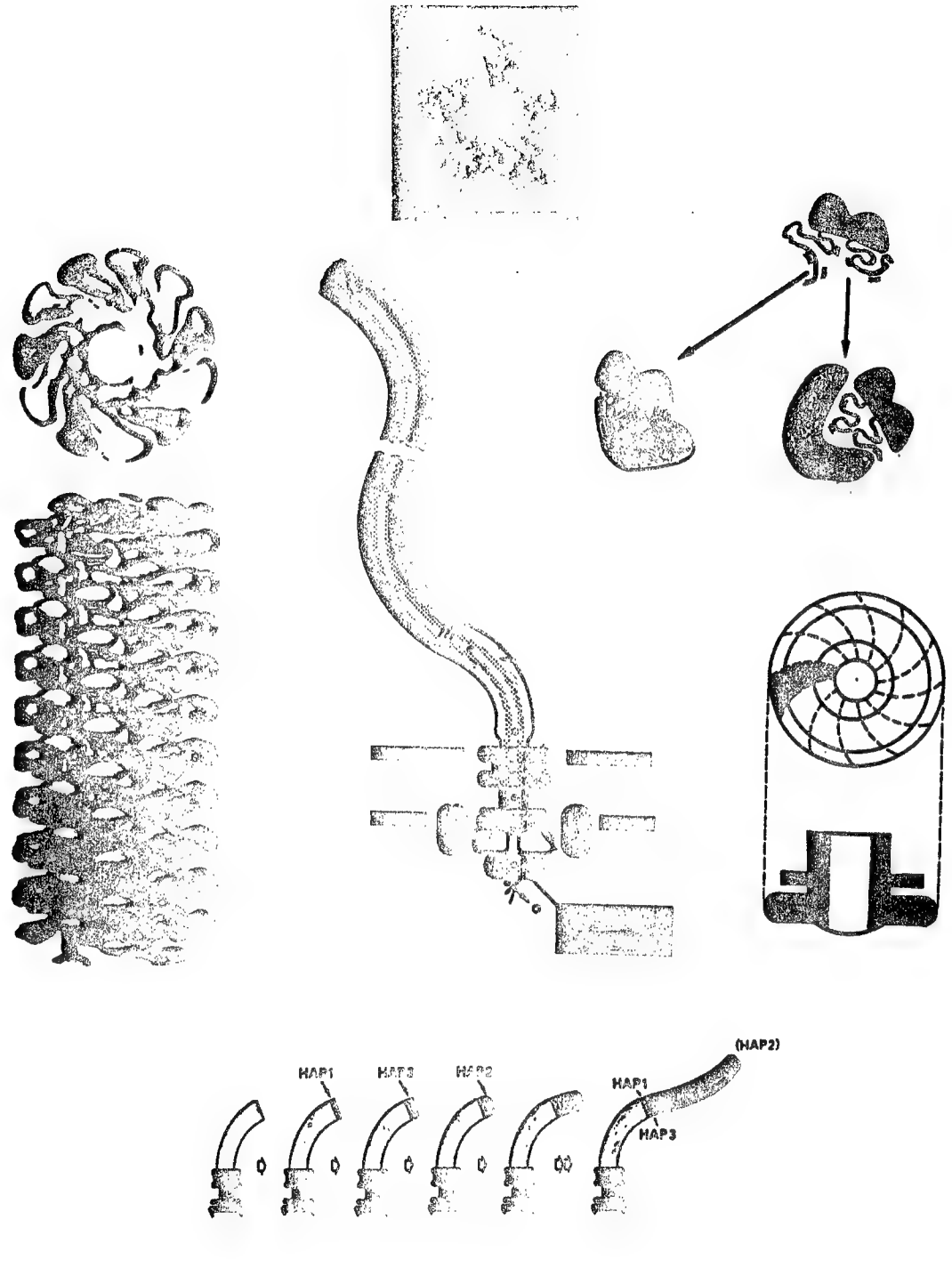
HAP1
HAP3
HAP2
HAP1
(HAP2)
HAP3

NOYORI MOLECULAR CATALYSIS PROJECT--From R..dy-Made to Tailor-Made Catalysts

OBJECTIVE Perfect chemical reactions

CONCEPT A well-designed single catalyst produces a single compound.

STRATEGY Molecular catalysis via organometallic chemistry

MOLECULAR CATALYSTS

Metal + Organic Ligand

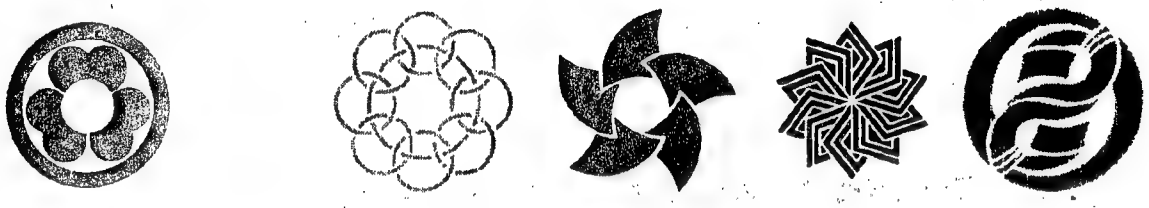

PROJECT ORGANIZATION

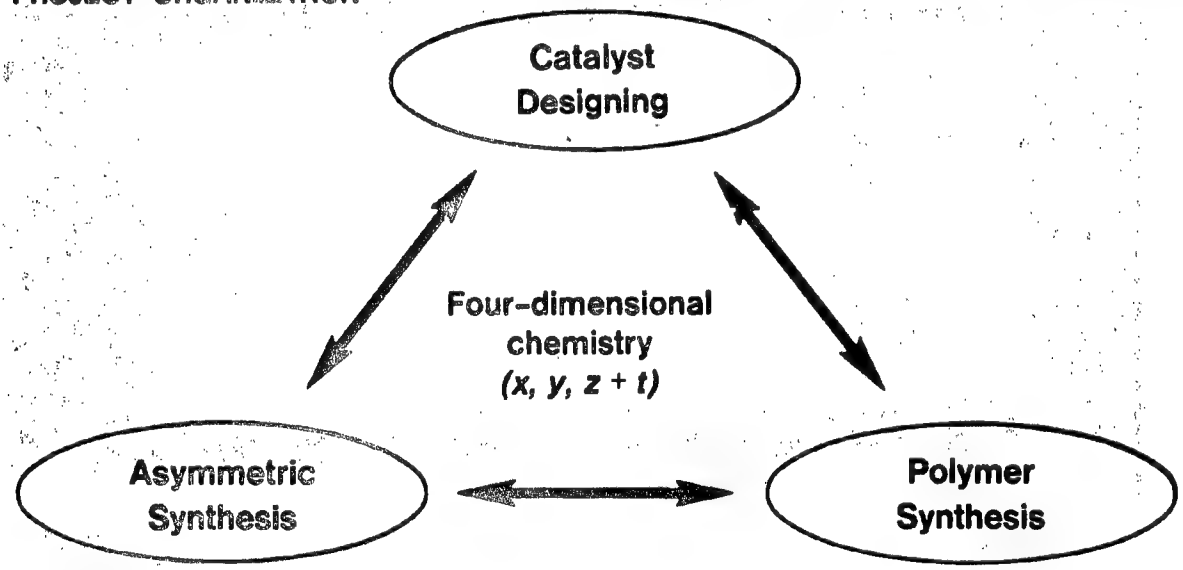

Targets

- Biologically active compounds
- Advanced materials

SELF AND NONSELF RECOGNITION OF ASYMMETRIC CATALYSTS

CHIRALITY AMPLIFICATION

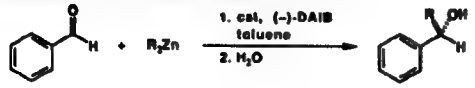

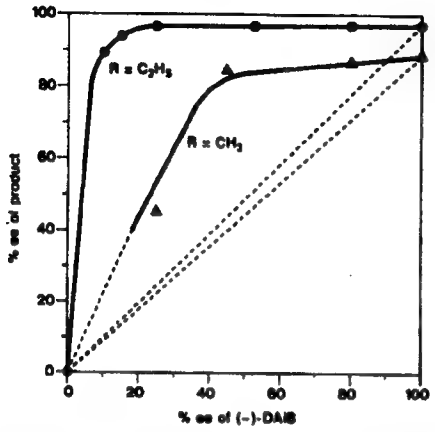

(-)-DAIB % ee	product (R = C_2H_5) % ee
100	98
15	95

(-)-DAIB =

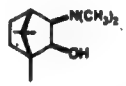

REACTION MECHANISM

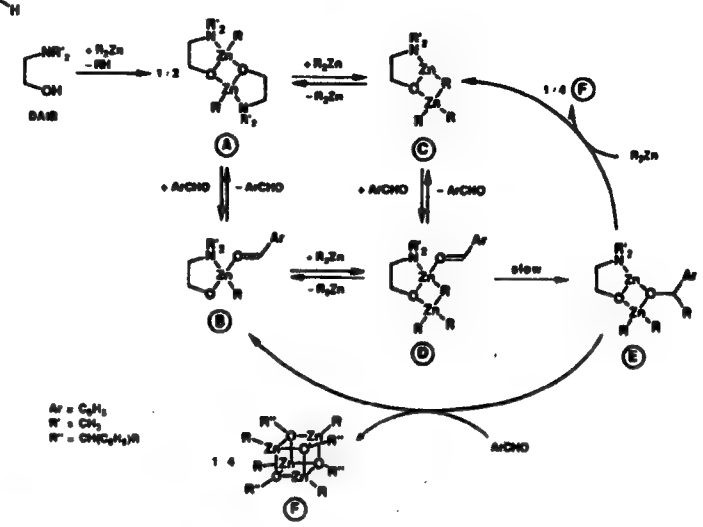

SELF AND NONSELF RECOGNITION OF CATALYSTS

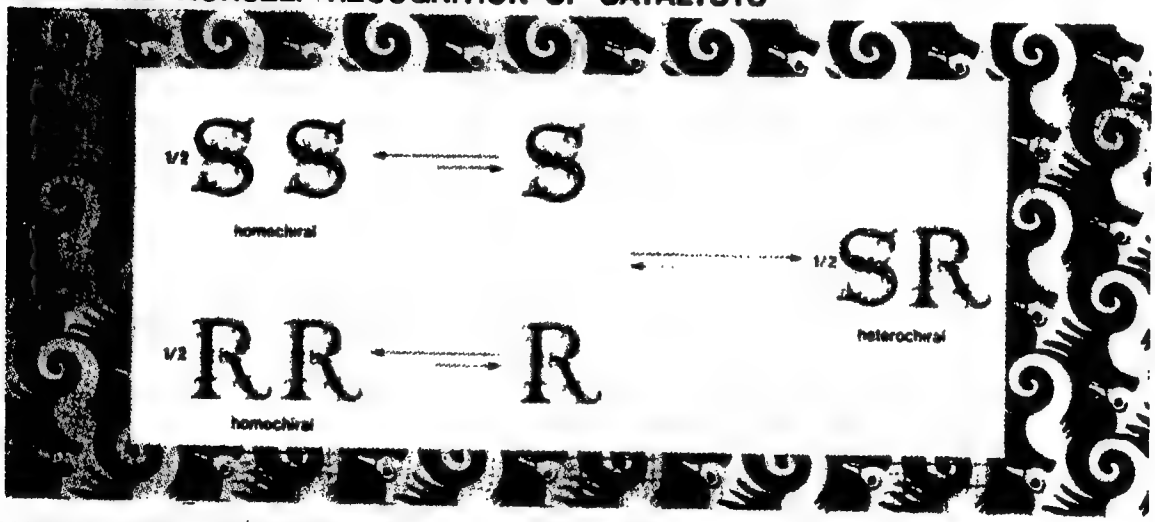

HOMOCHIRAL AND HETEROCHIRAL INTERACTION

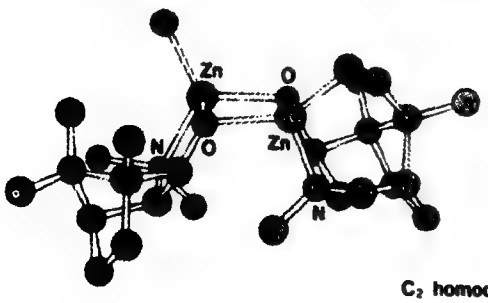

C_2 homochiral
reactive
ϕ (5/4)=140°

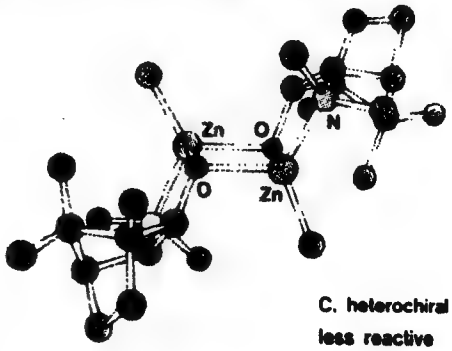

C. heterochiral
less reactive
ϕ (5/4)=120

ASYMMETRIC ISOMERIZATION OF ALLYLIC AMINES

TAKASAGO MENTHOL SYNTHESIS

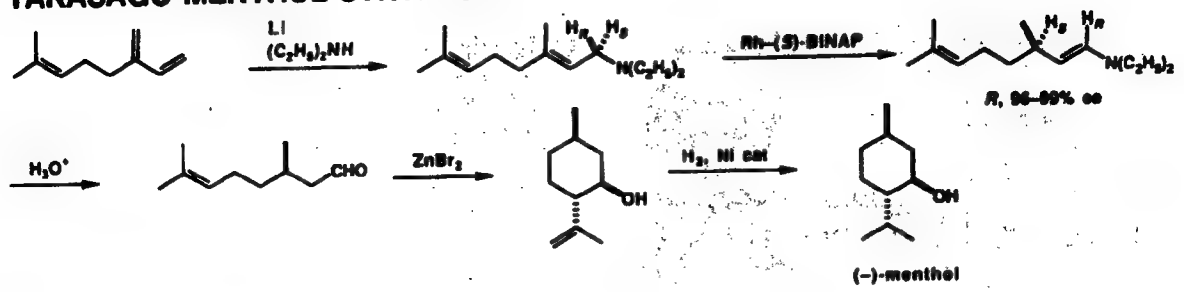

(–)-menthol

Catalyst (precursor)

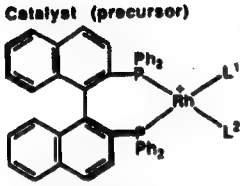

L^1, L^2 = THF, acetone

L^1–L^2 = COD, (S)-BINAP, η^3-enamine

Reactive intermediate

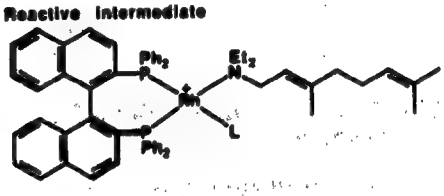

L = THF, acetone, η^1-enamine

AB INITIO CALCULATION

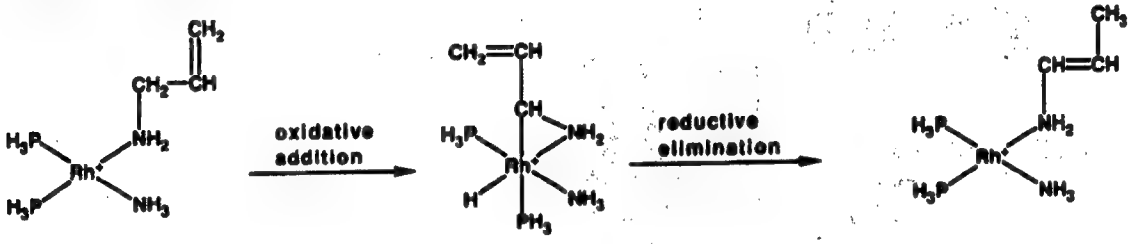

0.0 kcal/mol

–3.4

–4.9

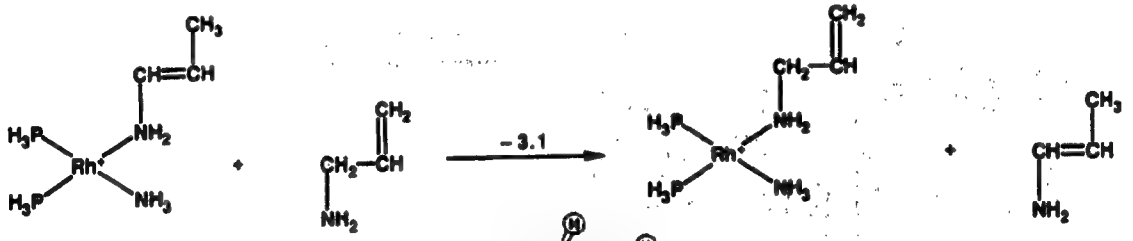

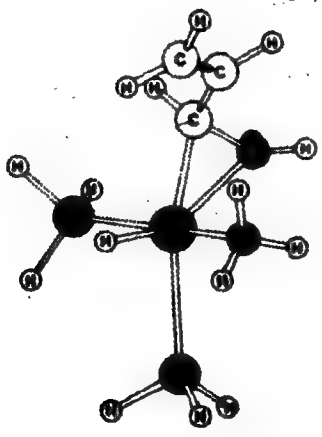

Rh(II) intermediate

PHOTORESPONSIVE CALIX[4]ARENES

Photoresponsive Calix[4]arenes

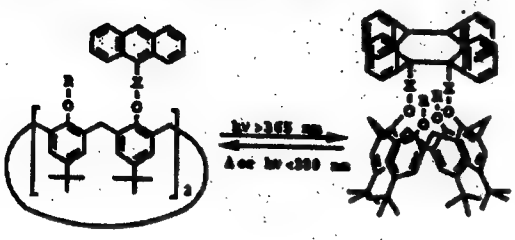

I II

	R	X
a	$-CH_2CH_2CH_3$	$-CH_2CO_2CH_2CH_2O$-(Ant)
b	$-CH_2CH_2OCH_2CH_3$	$-CH_2CH_2O$-(Ant)

Scheme 1. Structures of Photoresponsive Calix[4]arenes

Synthesis

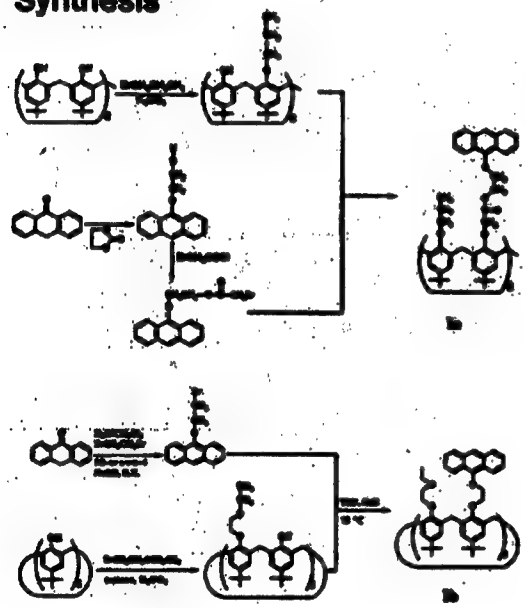

Scheme 2. Synthetic Routes to Bisdiazocene Linked Calix[4]arenes

Potential Applications

Photoswitchable Ion Sensor

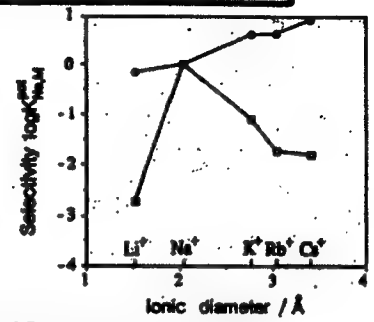

Figure 3. Photoresponsive ion selectivity as estimated by an electrochemical method : before irradiation(○) and after irradiation(□) in PVC.

Photoregulated Ion Conductance

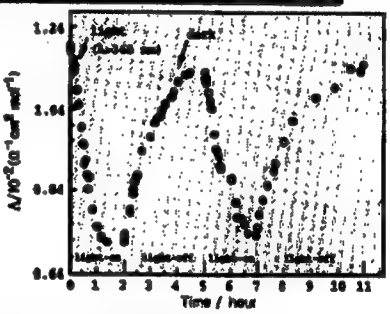

Figure 3. Photoresponsive conductivity change in THF. [I a] = 6.9 x 10^{-3} mol dm^{-3}, [$NaClO_4$] = 2.5 x 10^{-4} mol dm^{-3}.

Reversible Optical Memory

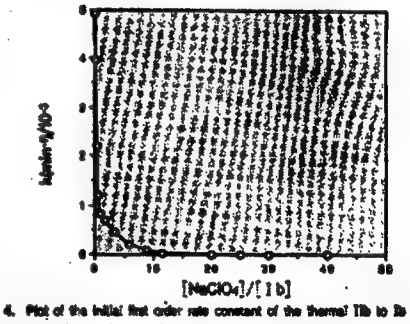

Figure 4. Plot of the initial first order rate constant of the thermal IIb to Ib conversion vs. the molar ratio of [$NaClO_4$] / [I b] within PVC membranes plasticized with di (2-ethyl hexyl) sebacate.

[continued]

[Continuation of Photoresponsive Calix[4]arenes]

Photodimerization

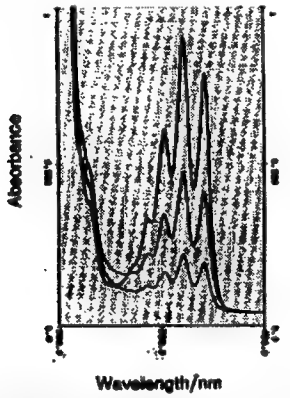

Figure 1. Reversible absorbance of Ib (0.6 wt%) within PVC membrane plasticized with di(2-ethylhexyl) sebacate in the molar ratio of [$NaClO_4$] / [Ib] = 20. Before irradiation(—); after 15 min irradiation at 361 nm(- - -) ; and further irradiated at 279 nm for 4 min(— - —).

Aqueous-Organic Two Phases Extraction

Table 1. Extractabilities (Ex%) of alkali picrate*

	Extractant			
Metal	Ia	IIa	Ib	IIb
Li^+	12.2	10.5	2.8	10.4
Na^+	48.8	4.9	11.8	61.4
K^+	2.1	3.0	2.0	2.9
Rb^+	4.3	2.7	2.0	2.0
Cs^+	1.0	1.0	2.0	2.0

* Organic phase : 5 ml CH_2Cl_2 [I] or [II] = 8.04×10^{-4} mol dm^{-3}. Aqueous phase : 5 ml water, [MOH] = 0.1 mol dm^{-3}, [MCl] = 0.5 mol dm^{-3}, [picrate acid] = 2.26×10^{-4} mol dm^{-3}. Extraction time: 30 min, -5°C.

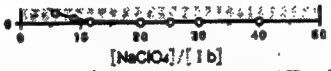

Figure 4. Plot of the initial first order rate constant of the thermal IIb to Ib conversion vs. the molar ratio of [$NaClO_4$] / [Ib] within PVC membranes plasticized with di (2-ethyl hexyl) sebacate.

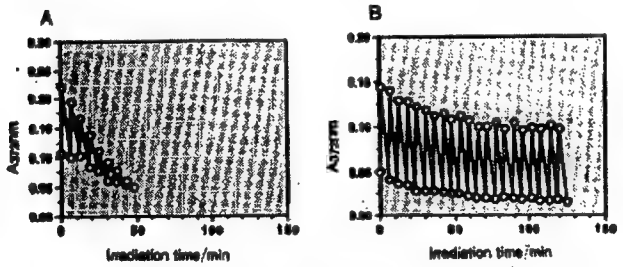

Figure 5. Photocycles of Ib without $NaClO_4$ (A) and with [$NaClO_4$] / [Ib] = 20 (B) in the PVC membranes plasticized with di (2-ethyl hexyl) sebacate. The membranes were first irradiated at 361 nm for 20 min. The following one cycle consists of alternate irradiation at 279 nm for 1 min and 361 nm for 5 min.

Conclusion

Research on the relationships between binding and external influences is an active field of supramolecular chemistry. The present work provides evidence that elucidates such relationships. These results will direct our future work in the construction of photoresponsive ion channels, and optical or electronic devices which use such host-guest interactions.

Specific Complexations of Saccharides With Diphenyl-3,3′-diboronic Acid That Can Be Detected by Circular Dichroism

—molecular recogniton of saccharides in an aqueous system—

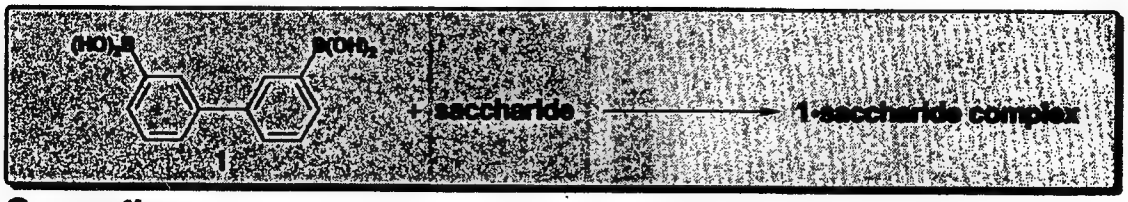

Conceptions

1. Specific complexation with disaccharides

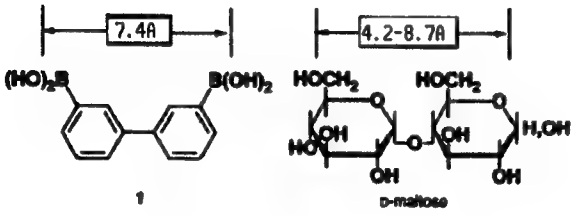

2. Formation of CD-active atrop isomers which reflect the structure of saccharides

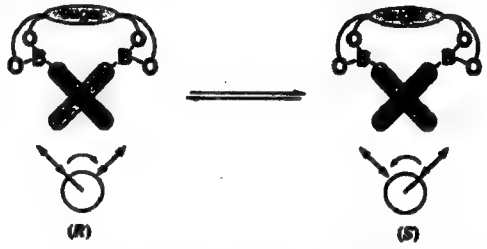

A pair of atrop isomers formed from 1 and saccharide

CD properties and association constants

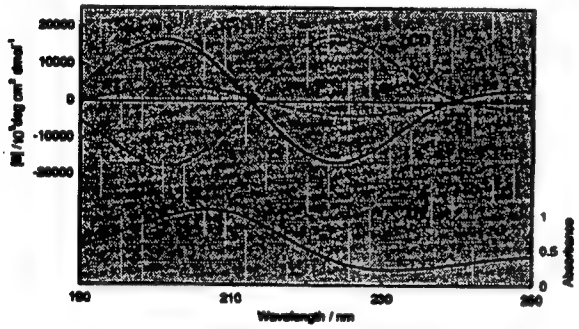

Figure. Absorption spectrum of 1 (6.0×10^{-5} mol dm^{-3}) and CD spectra of 1 (6.0×10^{-5} mol dm^{-3}) · disaccharide (6.0×10^{-5} mol dm^{-3}) complexes : — D-maltose, — — — D-cellobiose, · · · · D-lactose, 25°C, pH 10.5 with 0.1 mol dm^{-3} of carbonate buffer. At 180–200 nm region the precise CD measurement was difficult because of the strong background (shown as dotted lines)

Table. Absorption and CD spectra of 1 and its disaccharide complexes and their association constants (K)[a]

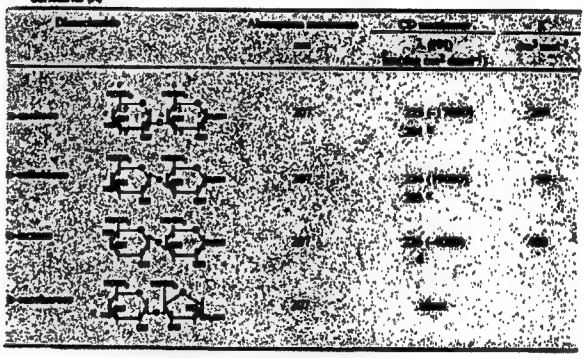

a 25°C, pH:10.5 with 0.1 mol dm^{-3} carbonate buffer.
b $[\theta]^1_{max}$ is positive, but $[\theta]$ could not be determined precisely.
c $[\theta]_{max}$ is negative, but $[\theta]$ could not be determined precisely.
d $[\theta]_{max}$ is positive, but $[\theta]$ and λ_{max} could not be determined precisely.

[continued]

[Continuation of Specific Complexations...]

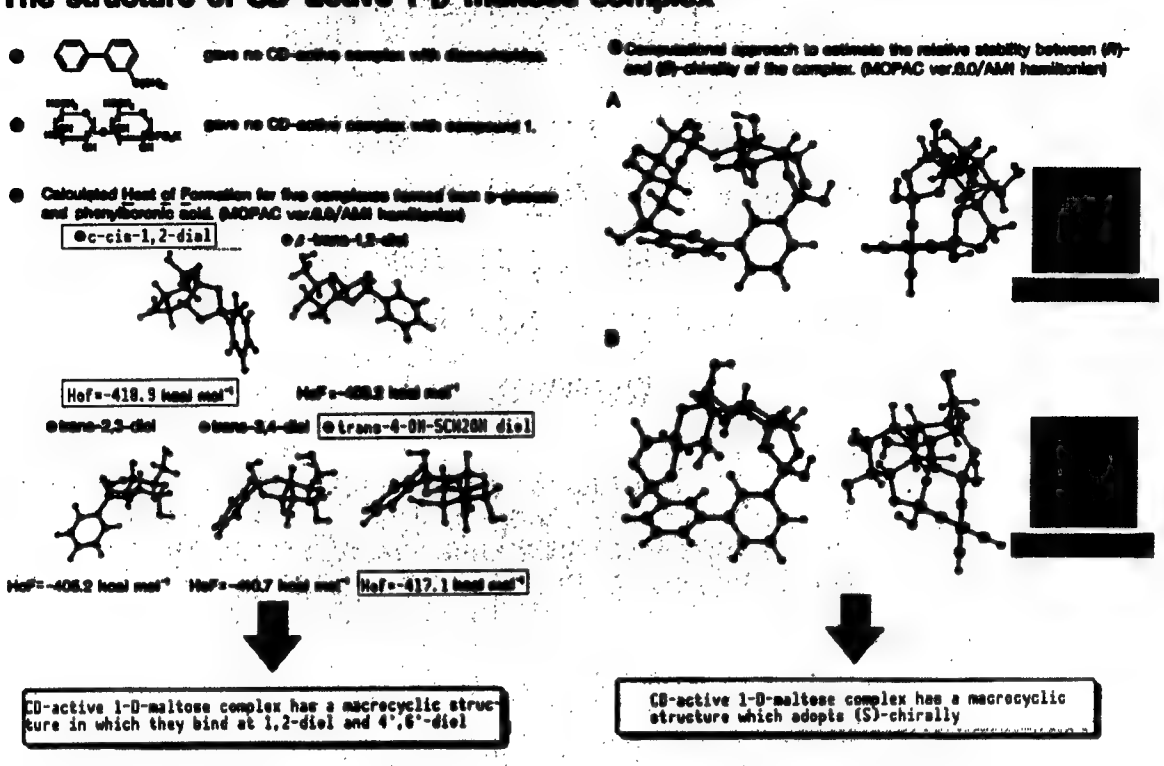

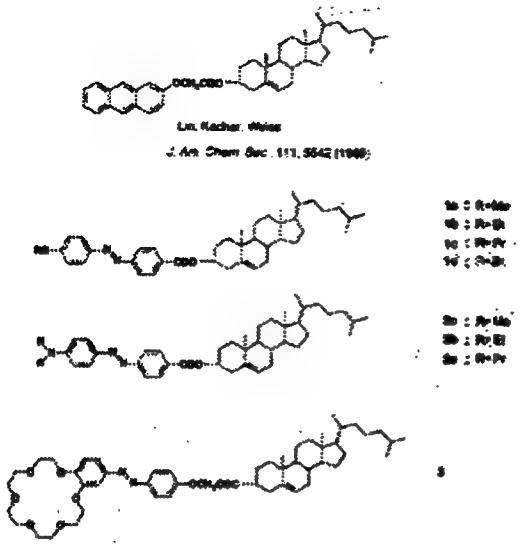

Figure 1. Cholesterol-based gelators

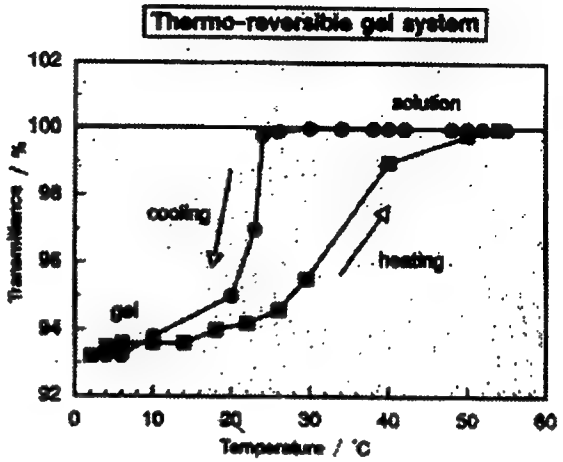

Figure 3. Temperature dependence of transmittance for 1a-butanol system on heating (×) and cooling (●); [1a] = 0.1 wt %.

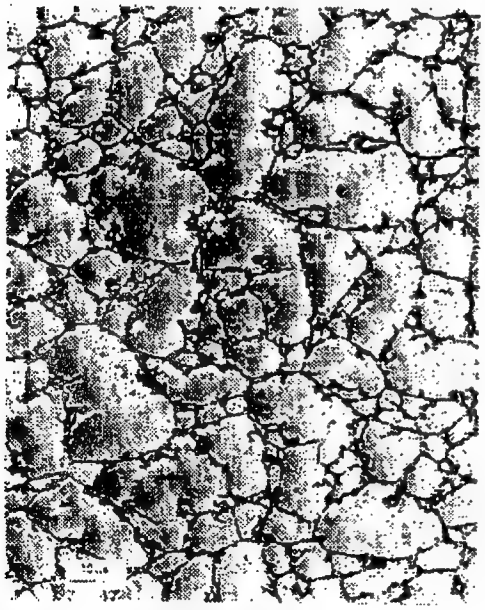

Figure 2. TEM of 3-methylcyclohexane/benzene (8/2 w/w%)

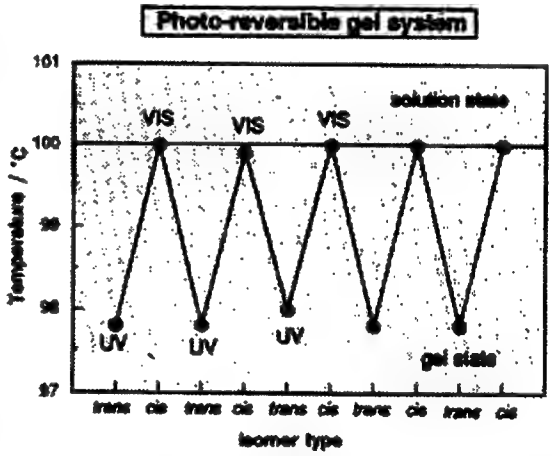

Figure 4. Photocontrol of the sol-gel phase transition for 1a-butanol system at 22°C; [1a] = 0.1 wt %; UV denotes irradiation of UV light (330< λ <380 nm) and VIS denotes irradiation of visible light (λ >460 nm).

[continued]

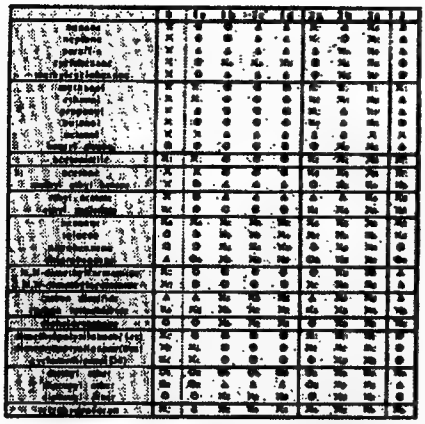

Table 1. Organic fluid tested for gelation; ○ : gel formed when cooled in water at 2-10°C and stable at room temperature (ca. 20-25°C), ○s : unstable at room temperature, (● : the concentration of the gelator under 1 wt %), △ : gel formed when cooled in a refrigerator (-6°C), (▲ : stable at room temperature), × : gel not formed (×c : recrystalized, ×i : insolved, ×s : solved)

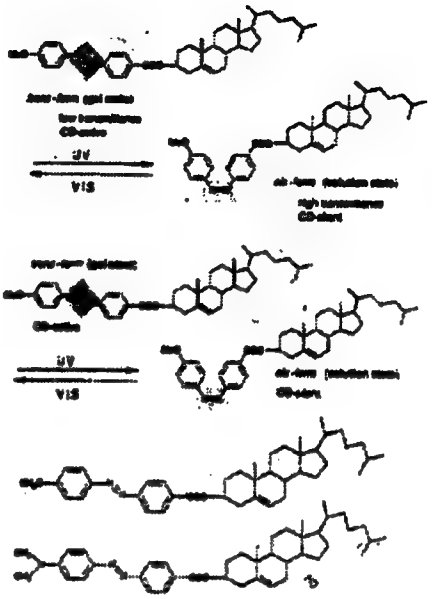

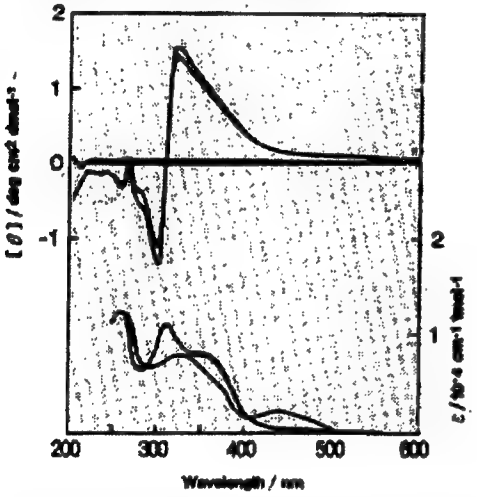

Figure 5. Photoinduced change of CD spectra (above) and absorption spectra (below) for a 1a-butanol system at 22°C ; [1a] = 0.2 wt % ; before UV irradiation (——), after UV irradiation (----), after VIS irradiation (-·-).

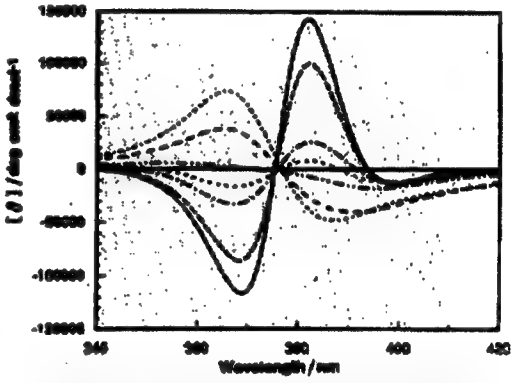

Figure 6. CD spectra for 2a-methylcyclohexane system on heating; [2a] = 0.5 wt % ; ——15°C, ---- 22°C, —·— 26°C, ···· 29°C, —··— 31°C, - - - 33°C, ·····- 37°C.

Microphotoconversion Project

October 1988 - September 1993

Project Director : Professor **Hiroshi Masuhara** (Osaka University)

Toward Integrated Microchemical Systems

Cascade Chemical Reactions are to be Conducted Sequentially along a Series of Spatially - Arranged Micrometer Reaction Sites

Research Groups

1. **Dynamic Microspectroscopy Group** (*In Kyoto Research Park, Kyoto*)
2. **Microchemical Function Group** (*In Cent. Res. Lab., Idemitsu Kosan Co. Ltd., Sodegaura*)
3. **Microconversion System Group** (*In Res. Inst. for Production Development, Kyoto*)

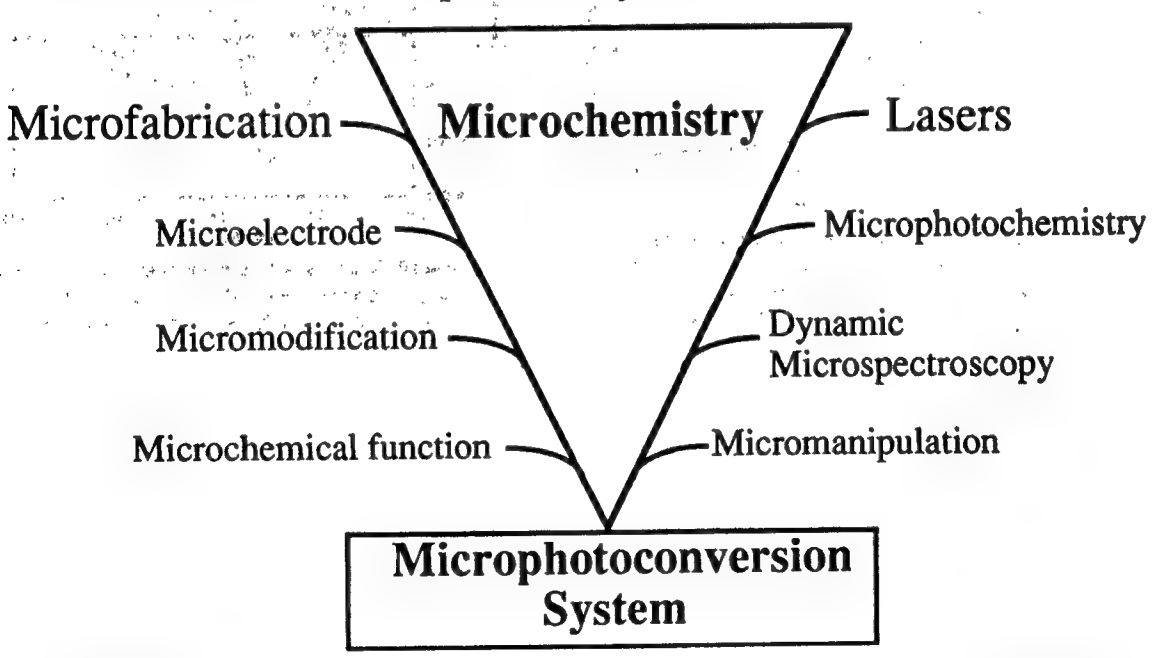

Exploratory Research for Advanced Technology (ERATO) Program
Research Development Corporation of Japan (JRDC)

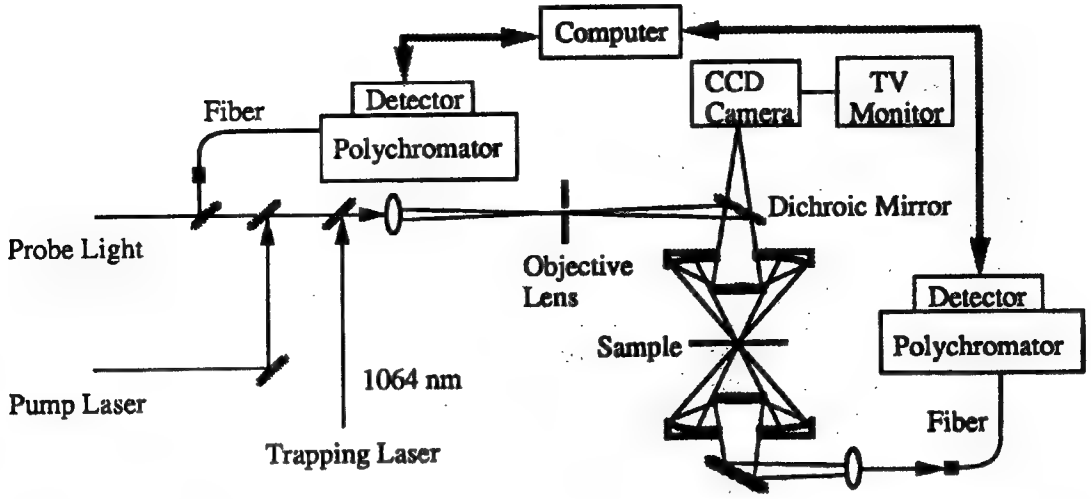

1. Subpicosecond transient absorption spectroscopy in small domains

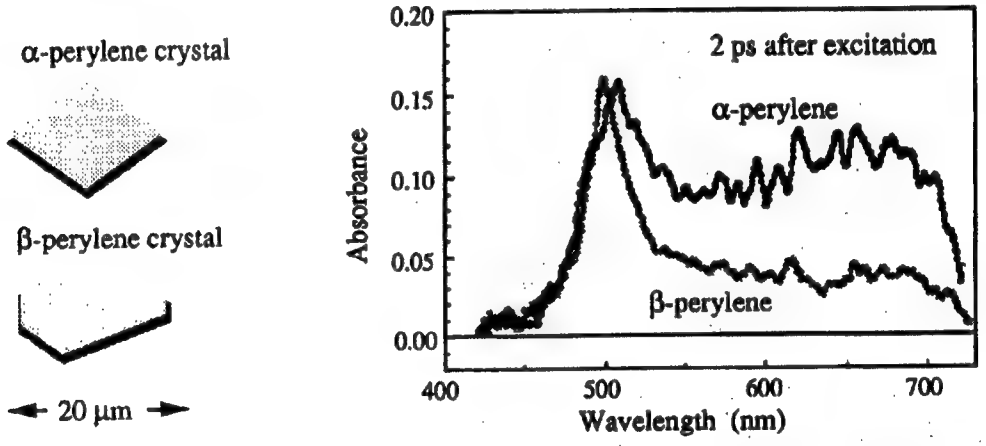

2. Transient absorption spectroscopy of a single liquid droplet

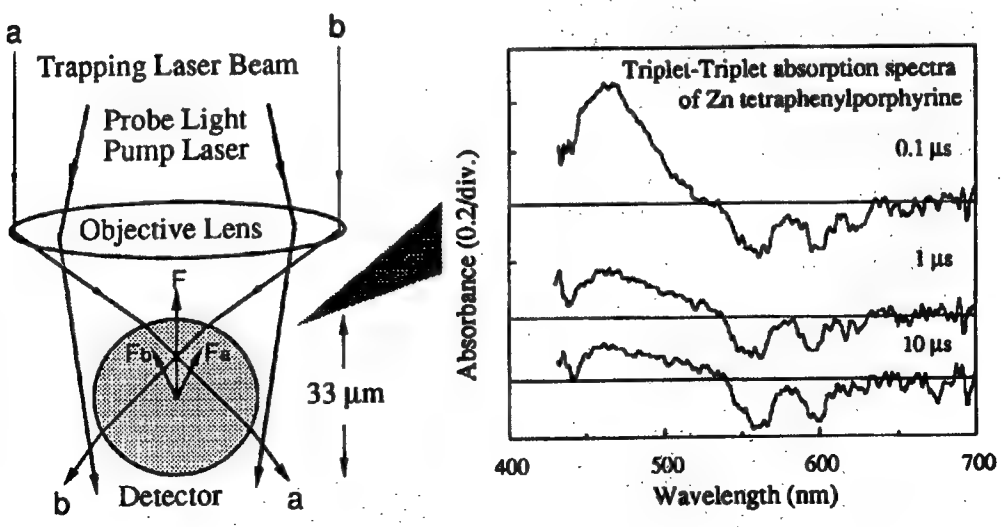

1. Principle of laser trapping

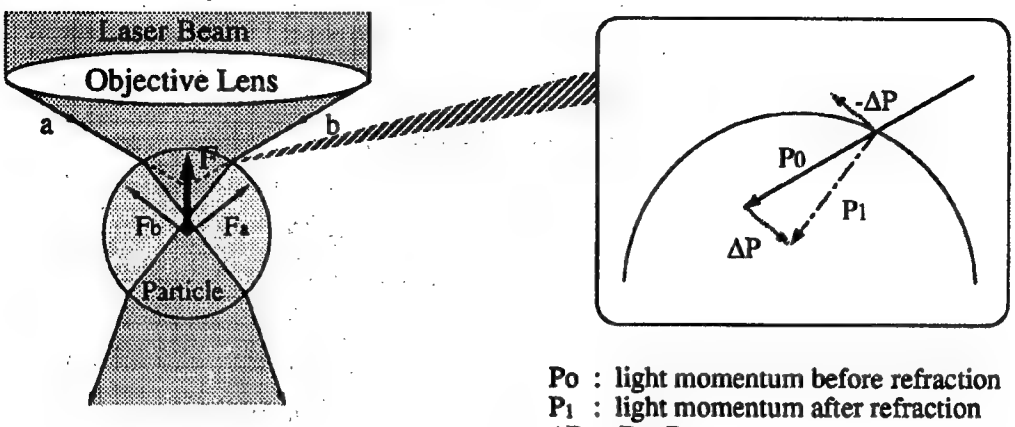

Po : light momentum before refraction
P_1 : light momentum after refraction
$\Delta P = P_1 - P_o$

2. Laser-scanning micromanipulation system

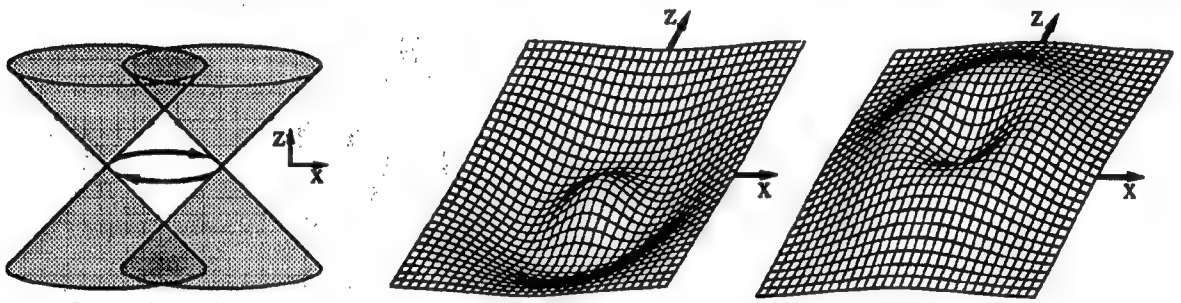

Scanning of Focused Laser Beam

$n_{Particle} > n_{medium}$

$n_{Particle} < n_{medium}$

n = Refractive Index

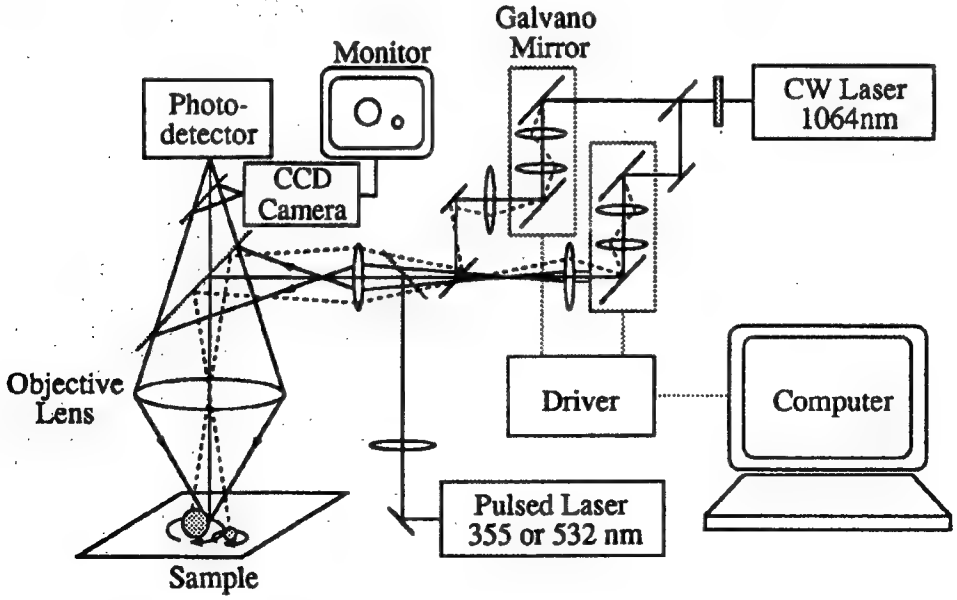

① Principle of STM

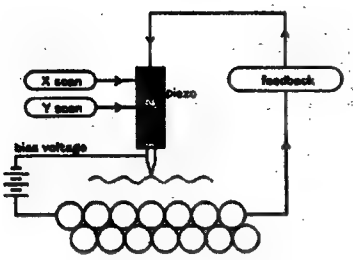

scan rate X : 1~2KHz
Y : 40Hz

② Azobenzene Derivative on Graphite

(1)wetting

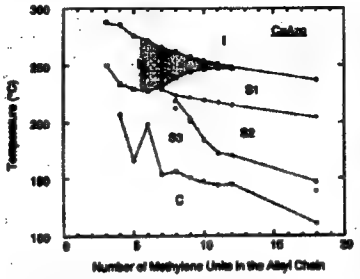

Graphite is wetted by nematic azobenzene LC but not by isotropic LC.

(2)STM Image

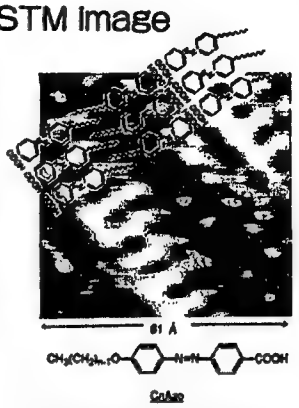

(head-to-head bilayer)

③ Epitaxial Monolayers of Polymers

(1) polyether

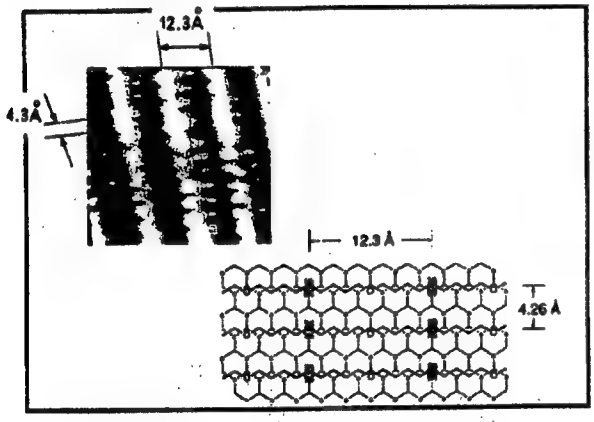

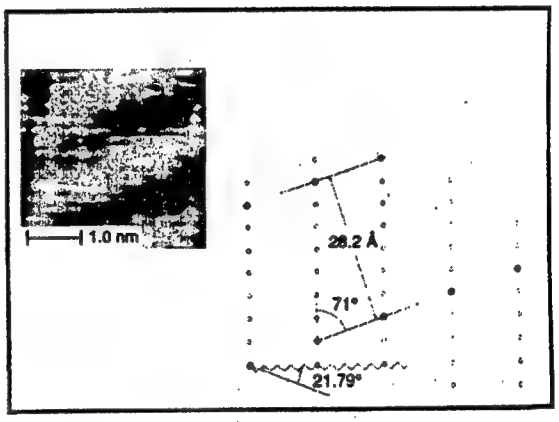

(2) polyester

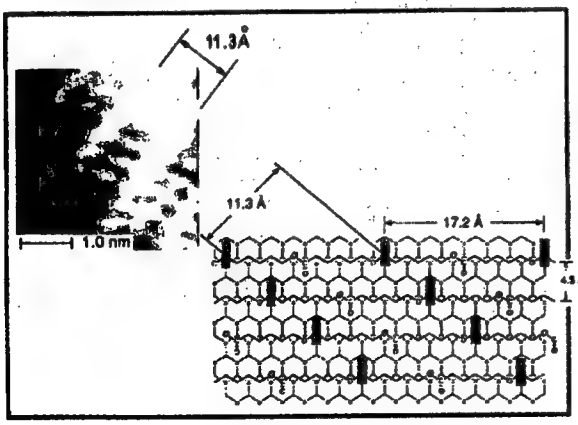

(3) nylon

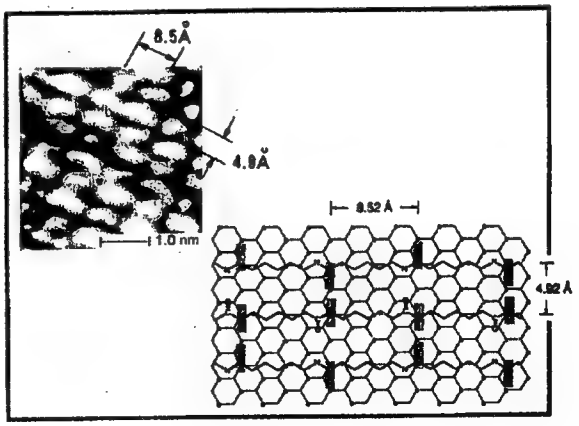

●Controlled Microstructures of Polysiloxane Films

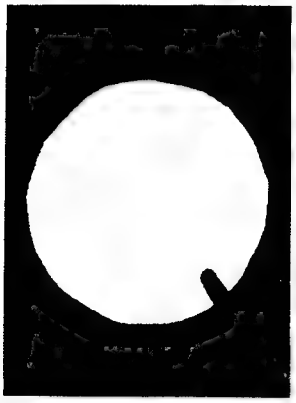

film(thickness 20μm)

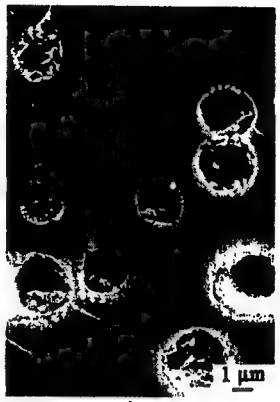

SEM view of film section

●Amine Derivatized Polysiloxane Film

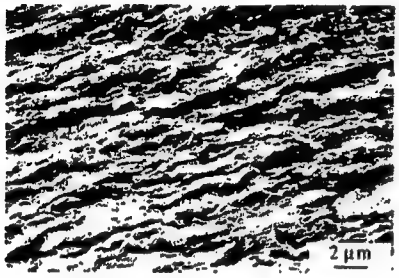

SEM view of cross section

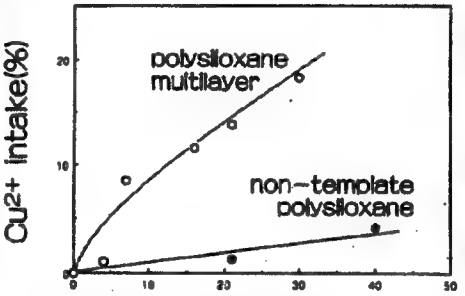

treatment with aq. Cu^{2+} (days)

●Silica-Alumina Ultrathin Film

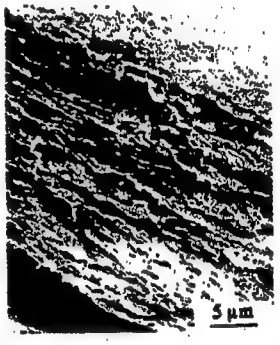

SEM view of cross section

● Ultrathin Film of Titania Particle

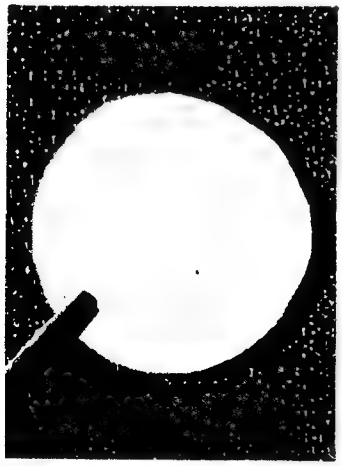

TiO_2 film (thickness 40μm)

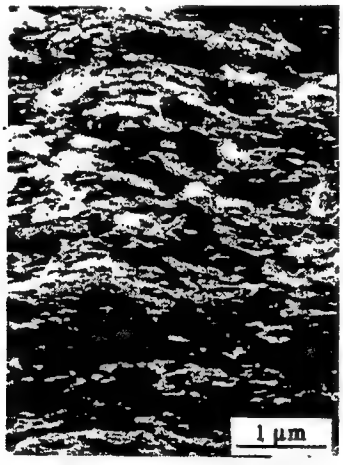

SEM view of film section

- Multilayer Film of 2D Cross-Linked Polymer (SEM view)

polyallylamine

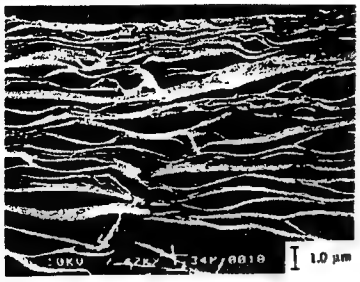

chitosan

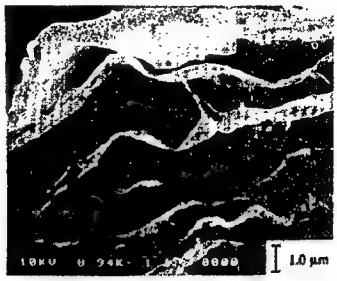

polyoxyethylene

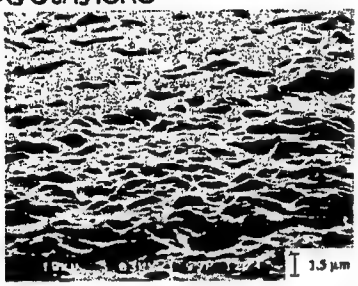

poly (tetraallylammonium bromide)

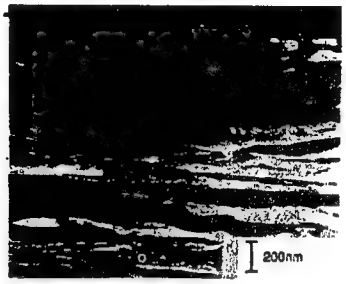

monomer : $CH_2=CHCO(CH_2CH_2O)_{14}CCH=CH_2$ (O, O)

- Regular Multilayer of Bilayer/Polymer Composite Film

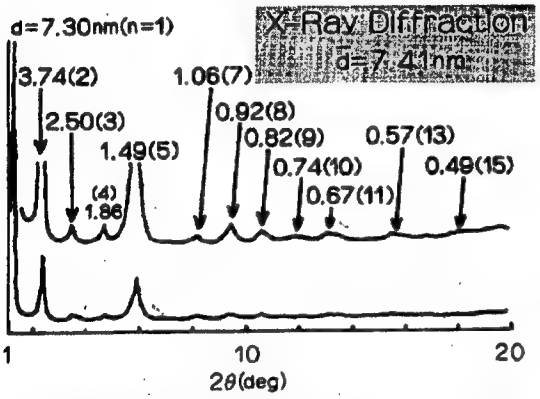

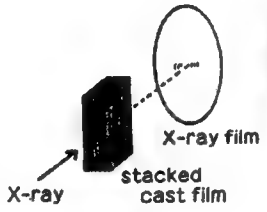

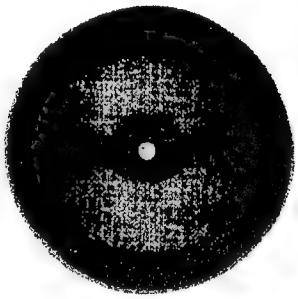

- Swelling of 2D-and 3D-Polyoxyethylenes

sample	Δa/a	Δb/b
2D polymer	0.15	0.69
3D polymer	0.13	0.12

- Mechanical Property of 2D- and 3D- Polyoxyethylenes

sample	tensile strength (kg/mm²)	modulus (kg/mm²)	elongation (%)
2D polymer	0.60	1.81	48
3D polymer	0.20	1.94	11

International Joint Research Program "Supermolecules," RDCJ
Universite Louis Pasteur (France)
Molecular Recognition and Supermolecule

① Molecular Recognition at the Air-Water Interface

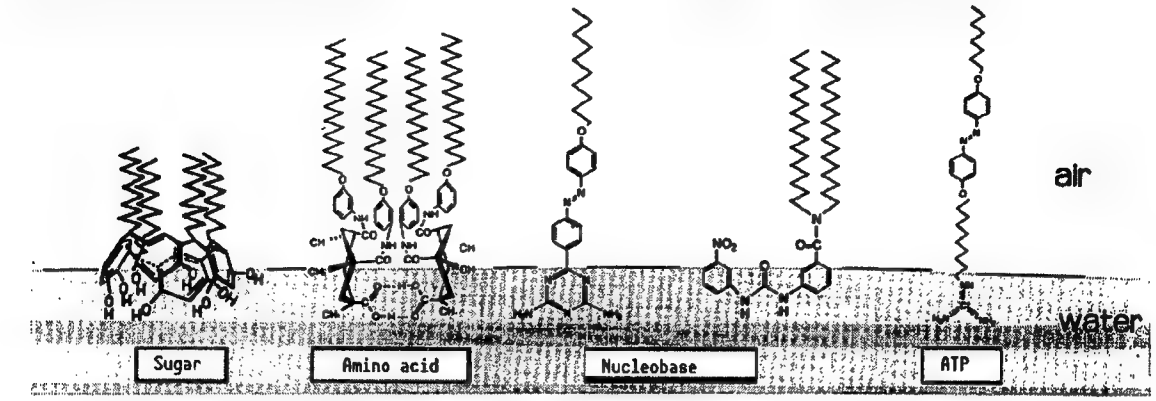

Substrate binding by hydrogen bonds

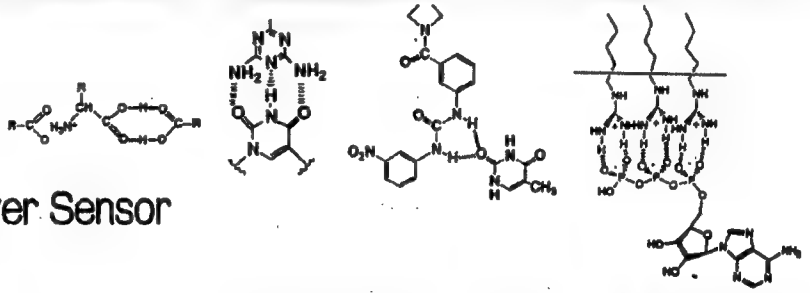

② Modified Monolayer Sensor

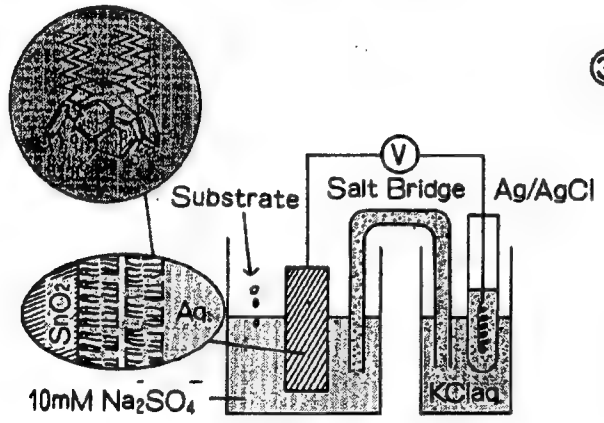

③ Monolayer of Non-cyclic Ionophore

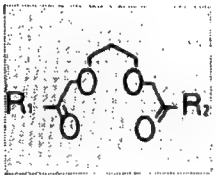

A: $R_1=R_2=$ $C_{18}H_{37}$ / CH_3 –N–

B: $R_1=(C_{18}H_{37})_2N-$, $R_2=(CH_3)_2N-$

C: $R_1=R_2=(C_{18}H_{37})_2N-$

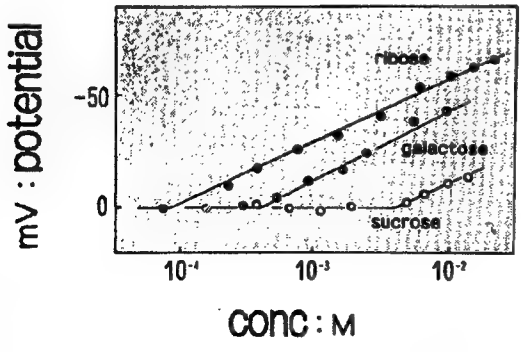

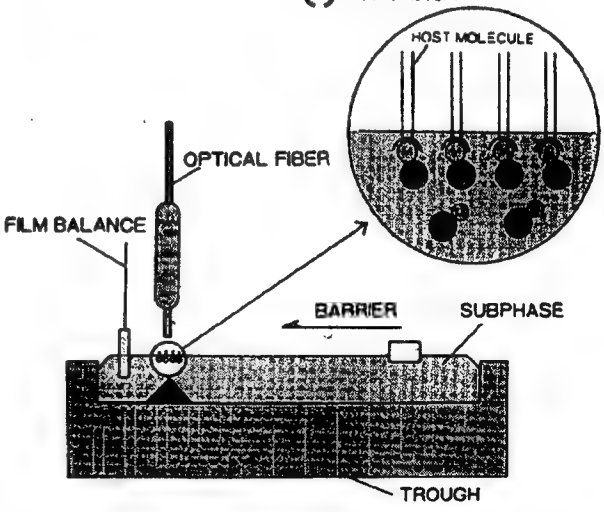

NAGAYAMA PROTEIN ARRAY PROJECT, ERATO, JRDC
- TOWARD THE SYNTHESIS OF HUMAN AND NATURAL TECHNOLOGY -

DIRECTOR: KUNIAKI NAGAYAMA, Ph.D.
GENERAL MANAGER, BIOMETROLOGY LAB, JEOL LTD.
PERIOD: OCTOBER 1990 - SEPTEMBER 1995

BACKGROUND

Throughout the long process of Earth's evaporation life has changed from relatively simple to highly sophisticated organisms by adopting the simple strategy of "protein assembly".

GOAL

Based on the molecular assembly capability of proteins, this project aims to fabricate macroscopic assembly structures, that is 2D protein arrays, useful for human beings. The highly regular structure of proteins should, therefore, allow us to control molecular alignment, crystal forms, and crystalline layers. Such efforts will lead to molecular devices in which proteins are used as constructive components.

STRATEGY

The principal strategy is to engineer proteins that favor specific inter-protein interactions and thus form integrated 2D arrays. Such microscopic engineering relies on mesoscopic colloid/surface forces. This is done by using theoretical approaches for conformational calculations and crystal simulations, as well as experimentally characterizating the crystallization process of protein and colloid particle arrays.

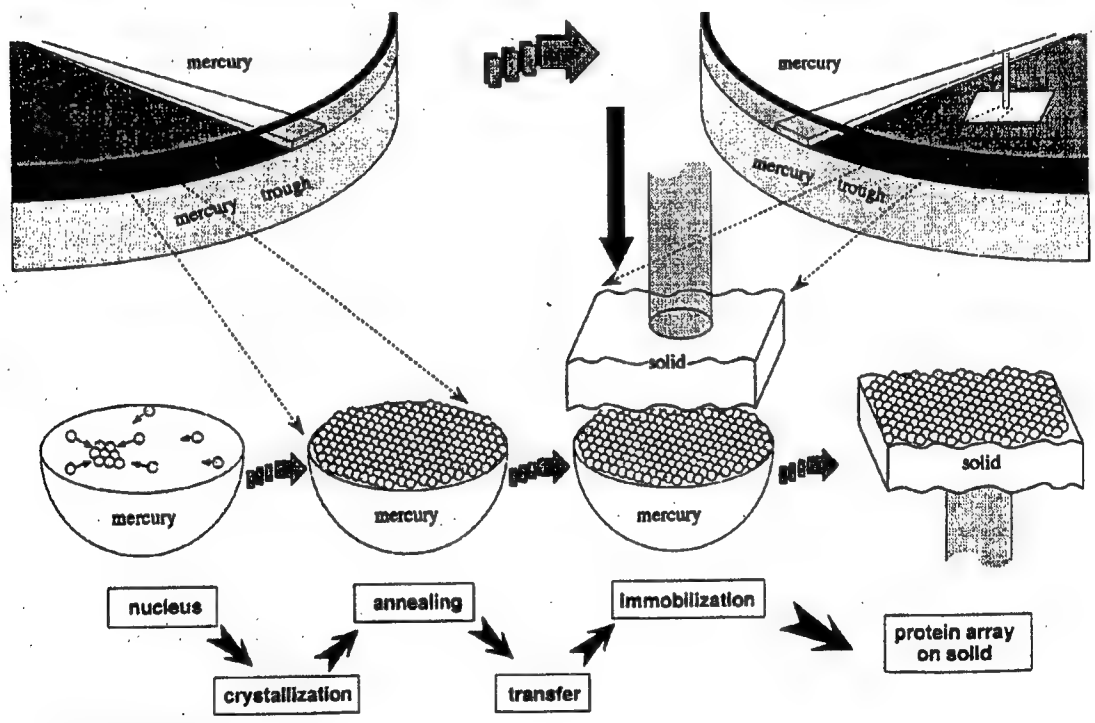

ORGANIZATION

The research task force consists of three groups, Array Design, Array Engineering, and Array Characterization.

Array Characterization Group

NAGAYAMA PROTEIN ARRAY PROJECT, ERATO, JRDC

LABORATORY: Tsukuba Research Consortium
Stanley Electric Co., Tsukuba

TASK MANAGER : Hideyuki Yoshimura, Ph.D., JEOL Ltd.

* FABRICATION OF PROTEIN AND MODEL PARTICLE 2D ARRAYS
* STATIC AND KINETIC STRUCTURAL CHARACTERIZATION OF 2D ARRAYS
* EXPERIMENTAL ANALYSIS OF THE ASSEMBLY MECHANISM

CURRENT TOPICS: (Ferritin and nanometers polystyrene particles are the primary targets)

* STATIC STRUCTURAL CHARACTERIZATION

Electron Crystallography (EC): Distinct integration patterns in the protein arrays are delineated by sophisticated EC with computer enhancement techniques.

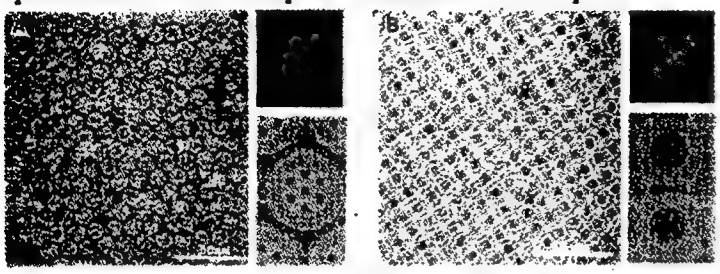

Electron Micrographs of Hexagonal (A) and Square Lattice Ferritin 2D crystals. Diffraction patterns and computer enhanced images are also shown.

Scanning Probe Microscopy (SXM): Atomic force microscopy (AFM) images are improved by using an electron beam deposition (EBD) microtip.

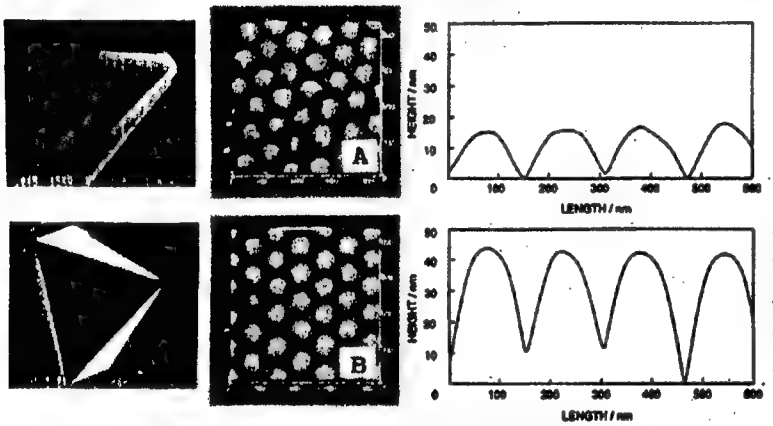

AFM Images of Polystyrene Particle Arrays using (A) a Commercial Cantilever and (B) an EBD-Tip.
The tip views are shown on the left and the image cross-sections are on the right, respectively.

* KINETIC STRUCTURAL CHARACTERIZATION

The synthesis of the microscopic design and the mesoscopic assembly can be depicted by real-time and precise in situ observation of the 2D assembly on a mercury surface. A combination of various optical means such as fluorescence- and ellipso-metry is necessarily adopted.

* FINE PARTICLE 2D ASSEMBLY MECHANISM IN A LIQUID THIN FILM

An ultra-long-range force, the lateral immersion force, governs the initial assembly process, nucleation.

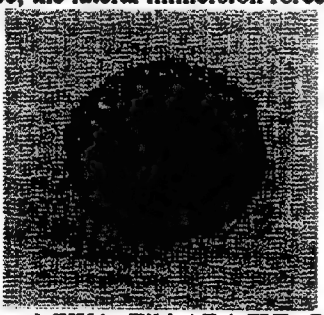

2D Assembly of Fine Particles with Two Distinct Diameters on a Mercury Surface. The larger particles dominantly gather at the center surrounded by the smaller ones due to the lateral immersion force in a liquid thin film (See the theoretical views in APPENDIX).

MEMBERS

Mariko YAMAKI, Tetsuya MIWA, Eiki ADACHI, Gilles PICARD, Tony DIMITROV (Tokyo Inst. of Technology, Univ. Trois Riviere, Sofia Univ.)

APPENDIX: LATERAL IMMERSION FORCE

NAGAYAMA PROTEIN ARRAY PROJECT
DESIGN GROUP

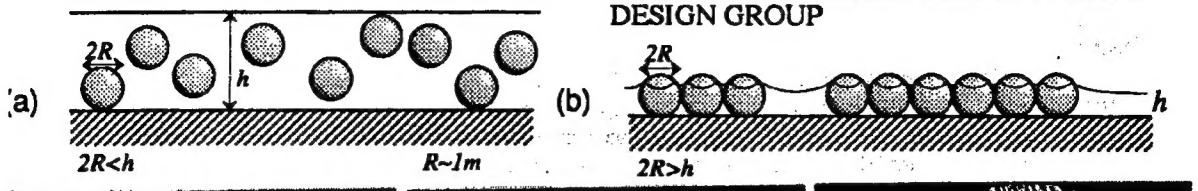

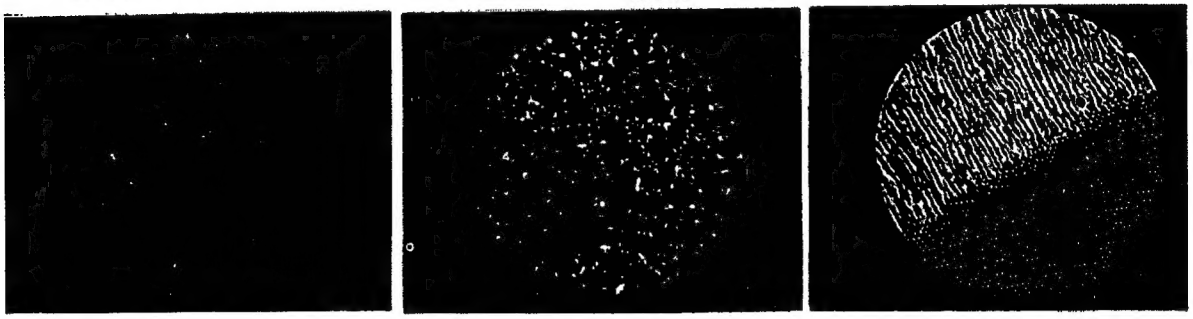

Brownian Motion

Particle ordering

LATERAL CAPILLARY FORCES

FLOTATION FORCES
due to particle weight
(plus Archimedes force)

effect driven by gravity

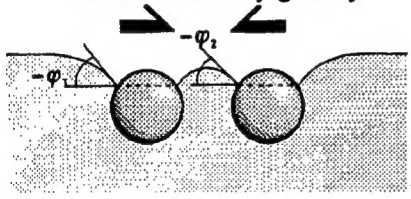

attraction

$\sin\varphi_1 \cdot \sin\varphi_2 > 0$

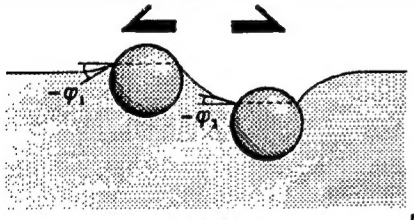

repulsion

$\sin\varphi_1 \cdot \sin\varphi_2 < 0$

flotation forces disappear for R < 10 μm

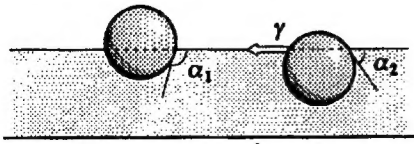

$F \propto \frac{1}{\gamma}$

IMMERSION FORCES
due to
capillary meniscus

effect driven by wetting

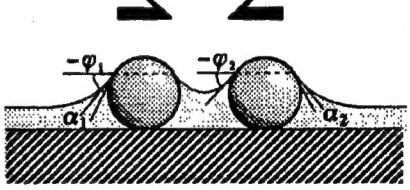

attraction

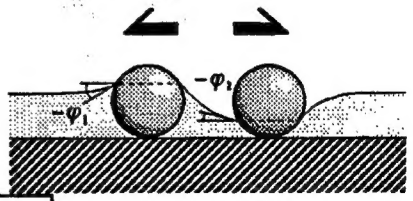

repulsion

immersion forces exist even for R ≈ 10 nm

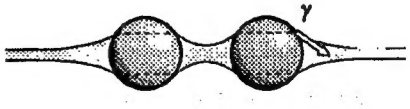

$F \propto \gamma$

Hotani Molecular Dynamic Assembly Project
Project director: Hirokazu Hotani (Teikyo University)

Overview

Biological organisms effectively perform highly sophisticated functions such as self-organization, self-replication, energy conversion and information processing. The unit elements which perform these intricate functions are thought to be assemblies of such biomolecules as proteins and lipids.

Molecular assemblies have been found to be capable of changing their own energy conversion and information transmission functions in response to environmental changes. Such assemblies are termed "supramolecules". Bacterial flagella, flagellar motors, microtubules and actin filaments have been mainly studied in our project.

The goal of the project is to understand why supramolecules function properly in thermally fluctuating environments and to explore related engineering applications. This could lead to the creation of "intelligent" molecular systems which auto-regulate their functions in response to circumstances and load.

1. Structural Analysis of Bacterial Flagella by X-ray Fiber Diffraction Method

Bacterial flagella are motile organelles and formed by assembly of subunit protein, flagellin. Flagellum adopts a number of distinct helical forms in response to environmental changes. To understand the molecular mechanism of the dynamic morphological transition, 3-D structure of flagellar filaments were obtained.

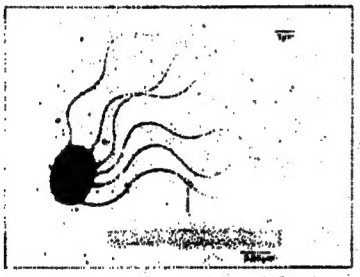

Electronmicrograph of a bacterium and its flagella

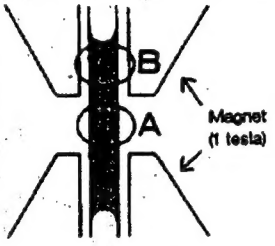

Orientation of flagellar filaments in high magnetic field

X-ray diffraction patterns obtained from A and B areas in Figure left

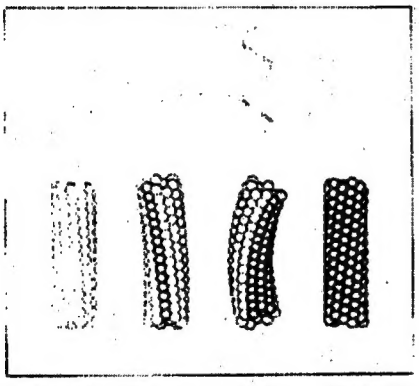

Model for polymorphism of bacterial flagella

X-ray fiber diffraction patterns

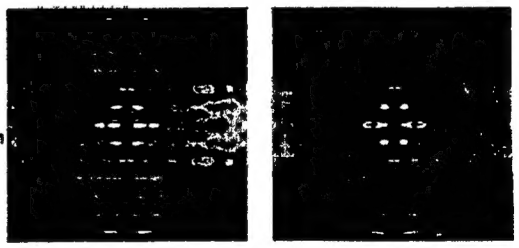

3-dimensional structure of bacterial flagella

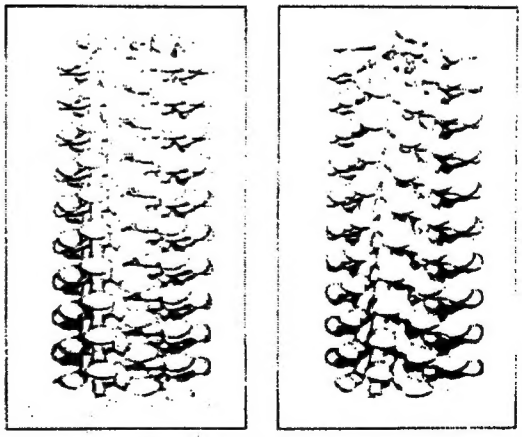

Small change in subunit conformation is responsible for regulating the morphology of a flagellar filament.

2. Formation of flagellar system

Subunit protein, flagellin, is transported to the distal end of a flagellum through a central channel and assembles there. A cap structure has a diameter of 10 nm, which is necessary in the assembly. The flagellar system was reconstituted in vitro.

Cap structure
scale: 10 nm

Schematic presentation of flagellin assembly at the tip of a flagellum

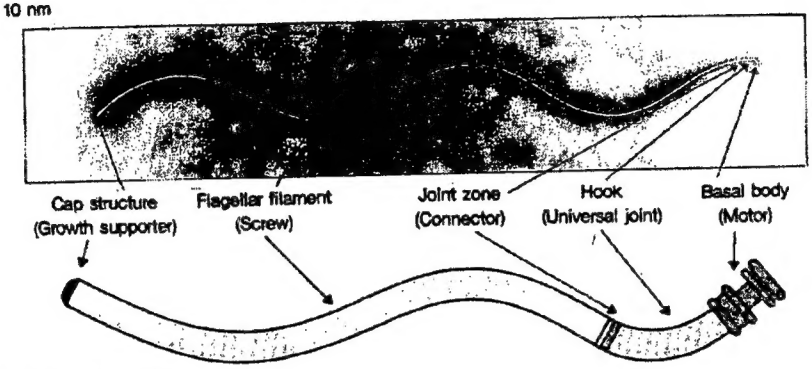

3. Control of a flagellar motor

A laser dark-field microscopy was developed, and it showed that a flagellar motor can rotate at 15,000 RPM. A single bacterium was trapped at the tip of a micropipette and the rotation speed was controlled by an external electric field.

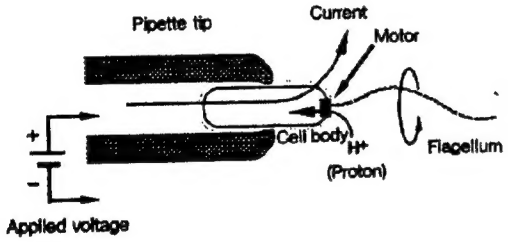

Phase contrast image

Dark-field image

A bacterium trapped at the tip of a micropipette

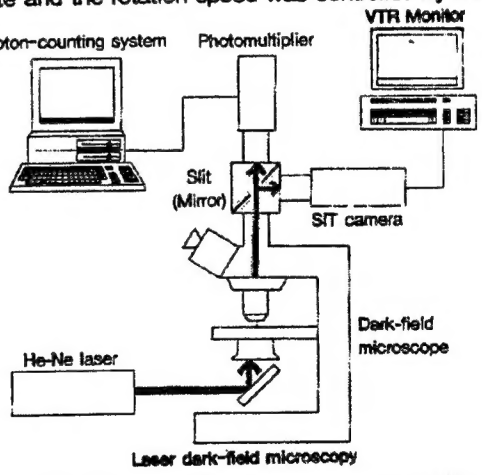

Laser dark-field microscopy

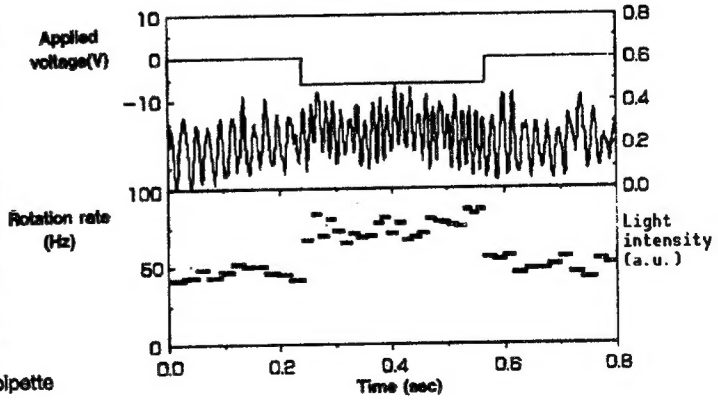

– END –

Foreign Broadcast Information Service (FBIS) and Joint Publications Research Service (JPRS) publications contain political, military, economic, environmental, and sociological news, commentary, and other information, as well as scientific and technical data and reports. All information has been obtained from foreign radio and television broadcasts, news agency transmissions, newspapers, books, and periodicals. Items generally are processed from the first or best available sources. It should not be inferred that they have been disseminated only in the medium, in the language, or to the area indicated. Items from foreign language sources are translated; those from English-language sources are transcribed. Except for excluding certain diacritics, FBIS renders personal names and place-names in accordance with the romanization systems approved for U.S. Government publications by the U.S. Board of Geographic Names.

Headlines, editorial reports, and material enclosed in brackets [ ] are supplied by FBIS/JPRS. Processing indicators such as [Text] or [Excerpts] in the first line of each item indicate how the information was processed from the original. Unfamiliar names rendered phonetically are enclosed in parentheses. Words or names preceded by a question mark and enclosed in parentheses were not clear from the original source but have been supplied as appropriate to the context. Other unattributed parenthetical notes within the body of an item originate with the source. Times within items are as given by the source. Passages in boldface or italics are as published.

SUBSCRIPTION/PROCUREMENT INFORMATION

The FBIS DAILY REPORT contains current news and information and is published Monday through Friday in eight volumes: China, East Europe, Central Eurasia, East Asia, Near East & South Asia, Sub-Saharan Africa, Latin America, and West Europe. Supplements to the DAILY REPORTs may also be available periodically and will be distributed to regular DAILY REPORT subscribers. JPRS publications, which include approximately 50 regional, worldwide, and topical reports, generally contain less time-sensitive information and are published periodically.

Current DAILY REPORTs and JPRS publications are listed in *Government Reports Announcements* issued semimonthly by the National Technical Information Service (NTIS), 5285 Port Royal Road, Springfield, Virginia 22161 and the *Monthly Catalog of U.S. Government Publications* issued by the Superintendent of Documents, U.S. Government Printing Office, Washington, D.C. 20402.

The public may subscribe to either hardcover or microfiche versions of the DAILY REPORTs and JPRS publications through NTIS at the above address or by calling (703) 487-4630. Subscription rates will be provided by NTIS upon request. Subscriptions are available outside the United States from NTIS or appointed foreign dealers. New subscribers should expect a 30-day delay in receipt of the first issue.

U.S. Government offices may obtain subscriptions to the DAILY REPORTs or JPRS publications (hardcover or microfiche) at no charge through their sponsoring organizations. For additional information or assistance, call FBIS, (202) 338-6735,or write to P.O. Box 2604, Washington, D.C. 20013. Department of Defense consumers are required to submit requests through appropriate command validation channels to DIA, RTS-2C, Washington, D.C. 20301. (Telephone: (202) 373-3771, Autovon: 243-3771.)

Back issues or single copies of the DAILY REPORTs and JPRS publications are not available. Both the DAILY REPORTs and the JPRS publications are on file for public reference at the Library of Congress and at many Federal Depository Libraries. Reference copies may also be seen at many public and university libraries throughout the United States.